Geochemistry Geophysics Geosystems G3
AN ELECTRONIC JOURNAL OF THE EARTH SCIENCES
Published by AGU and the Geochemical Society

Article
Volume 7, Number 4
12 April 2006
Q04004, doi:10.1029/2005GC001005
ISSN: 1525-2027

Trace element composition of mantle end-members: Implications for recycling of oceanic and upper and lower continental crust

Matthias Willbold and Andreas Stracke

Max-Planck-Institut für Chemie, Postfach 3060, D-55020 Mainz, Germany (willbold@mpch-mainz.mpg.de; stracke@mpch-mainz.mpg.de)

[1] Recycling of oceanic crust together with different types of marine sediments has become somewhat of a paradigm for explaining the chemical and isotopic composition of ocean island basalts. New high-precision trace element data on samples from St. Helena, Gough, and Tristan da Cunha, in addition to recent data from the literature, show that the trace element and isotope systematics in enriched mantle (EM) basalts are more complex than previously thought. EM basalts have some common characteristics (e.g., high Rb/La, Ba/La, Th/U, and Rb/Sr and low Nb/La and U/Pb) that distinguish them from HIMU basalts (high $\mu = {}^{238}U/{}^{204}Pb$). The isotopically distinct EM-1 and EM-2 basalts, however, cannot be clearly distinguished on the basis of incompatible trace element ratios. Ultimately, each suite of EM basalts carries its own specific trace element signature that must reflect different source compositions. In contrast, HIMU basalts show remarkably uniform trace element ratios, with a characteristic depletion in incompatible trace elements (Rb, Ba, Th, U, and Pb) and enrichment in Nb and Ta relative to EM basalts. Compositional similarities between HIMU and EM basalts (e.g., Nb/U, La/Sm, La/Th, Sr/Nd, Ba/K, and Rb/K) suggest that their sources share a common precursor, most likely recycled oceanic lithosphere. The compositional differences between HIMU and EM basalts, on the other hand, can only be explained if the EM sources contain an additional heterogeneous component. Parent-daughter ratios in subducted marine sediments have a unimodal distribution. Recycling of sediments alone can therefore not account for the isotopic bimodality of EM basalts. The upper and lower continental crust have similarly variable trace elements ratios but are systematically distinct in their Rb/Sr, U/Pb, Th/Pb, and Th/U ratios. Thus the upper and lower continental crust evolve along two distinct isotopic evolution paths but retain their complex trace element characteristics, similar to what is observed in EM basalts. We therefore propose that recycling of oceanic lithosphere together with variable proportions of lower and upper continental crust, which are introduced into the mantle together with the oceanic lithosphere via subduction erosion and/or subduction of marine sediments, respectively, provides a plausible explanation for the trace element and isotope systematics in ocean island basalts.

Components: 18,450 words, 18 figures, 3 tables, 1 dataset.

Keywords: lower continental crust; mantle heterogeneity; marine sediments; radiogenic isotopes; subduction erosion; trace elements.

Index Terms: 1025 Geochemistry: Composition of the mantle; 1040 Geochemistry: Radiogenic isotope geochemistry.

Received 25 April 2005; **Revised** 15 November 2005; **Accepted** 4 January 2006; **Published** 12 April 2006.

Willbold, M., and A. Stracke (2006), Trace element composition of mantle end-members: Implications for recycling of oceanic and upper and lower continental crust, *Geochem. Geophys. Geosyst.*, *7*, Q04004, doi:10.1029/2005GC001005.

1. Introduction

[2] On the basis of their isotopic composition, *White* [1985] and *Zindler and Hart* [1986] classified ocean island basalts (OIB) into three isotopically different families or groups: HIMU (= high μ, $\mu = {}^{238}U/{}^{204}Pb$) and two varieties of enriched mantle (EM-1 and EM-2; Figure 1). *Weaver* [1991] argued that each of these isotopic groups has certain common trace element characteristics that distinguish them from one another and so substantiated this classification. Thus, by the early 1990s an apparently coherent picture emerged. Recycling of oceanic crust with different types of sediment was favored as the most plausible explanation for the isotope and trace element systematics in oceanic basalts (pure oceanic crust for HIMU, oceanic crust plus "pelagic" sediment for EM-1 and oceanic crust plus "terrigenous" sediment for EM-2). In the meantime, however, the trace element database of global OIB has more than quadrupled and the quality of the trace element data has improved significantly. In addition, new data on subducted marine sediments have expanded our knowledge of their chemical variability [*Plank and Langmuir*, 1998]. Here, we reassess the global trace element systematics in oceanic basalts on the background of the isotope relationships observed in OIB, using new high-quality trace element data for OIB from several key islands: St. Helena, Tristan da Cunha (referred to as Tristan in the following) and Gough, in addition to recent data from the literature. This comprehensive data set now allows more rigorous testing of the sediment recycling model.

[3] It is shown here that HIMU basalts have very similar trace element compositions and likely derive from one common source reservoir. Despite the fact that there are some characteristics common to all EM basalts, each suite of EM basalts has its own unique trace element composition, which distinguishes it from any other suite of EM basalts. The trace element systematics of EM basalts therefore do not support grouping into two different types, EM-1 and EM-2, as suggested by the isotopic relationships, nor can any other grouping be identified. Is it justified therefore to maintain the distinction between only two types of EM basalts on the basis of their isotopic characteristics only, or do the trace element systematics indicate that EM sources are best evaluated by considering each island chain/group individually? Moreover, how can sources with similar time-integrated parent/daughter ratios but apparently different trace element signatures be produced, and is it conceivable that such sources share a similar genetic origin? In other words, the general question that arises from our analysis of the trace element systematics in OIB is: How can the isotope and trace element systematics in oceanic basalts be reconciled?

2. Data Set

[4] In addition to our newly determined data on samples from St. Helena, Tristan and Gough (Table 1, see Appendix A for analytical details), the overall data set includes data on more than 350 basalts from 15 ocean islands representing all major OIB families (HIMU, EM-1 and EM-2). The literature data were taken from the GEOROC database using the precompiled files made available at http://georoc.mpch-mainz.gwdg.de/georoc/. The final data set is restricted to samples from those islands of each island group/chain with the most extreme isotopic composition (Figure 1) and is available from the auxiliary material[1]. HIMU basalts are from St. Helena in the Atlantic Ocean, and from the islands of Mangaia, Tubuaii, and Rurutu (young and old series) of the Cook-Austral chain. EM-1 basalts are from Pitcairn Island, in addition to our new data for samples from Gough and Tristan. EM-2 basalts are from the Marquesas (Tahuata and Ua Pou), the Samoan Islands (Malumalu and Savaii), and the Society Islands (Tahaa, Moorea, and Hauhine). In addition, samples from the Azores (Sao Miguel) are included.

[5] From these preselected localities, only samples with major and trace element concentrations determined on the same sample (with the exception of some of the Society samples) were included in the final data set. These samples were further screened to exclude highly differentiated and altered rocks. In general, the cut-off for highly differentiated samples is chosen at a sharp decrease in CaO, FeO, and TiO_2 and increase in SiO_2 and Na_2O with decreasing MgO concentrations. As a result, only samples containing more than about 4 to 5 wt.% MgO are included in the final data set. All samples are alkaline rocks belonging to the alkali-olivine-basalt series [*Irvine and Baragar*, 1971]. With a few exceptions, the final data set includes only fresh samples with a "loss on ignition" (LOI) of less than 2%. The coherent behavior of fluid-mobile (e.g., Rb, K, U) and fluid-immobile elements (e.g., Th, Nb) was used as another proxy for

[1] Auxiliary material is available at ftp://ftp.agu.org/apend/gc/2005gc001005.

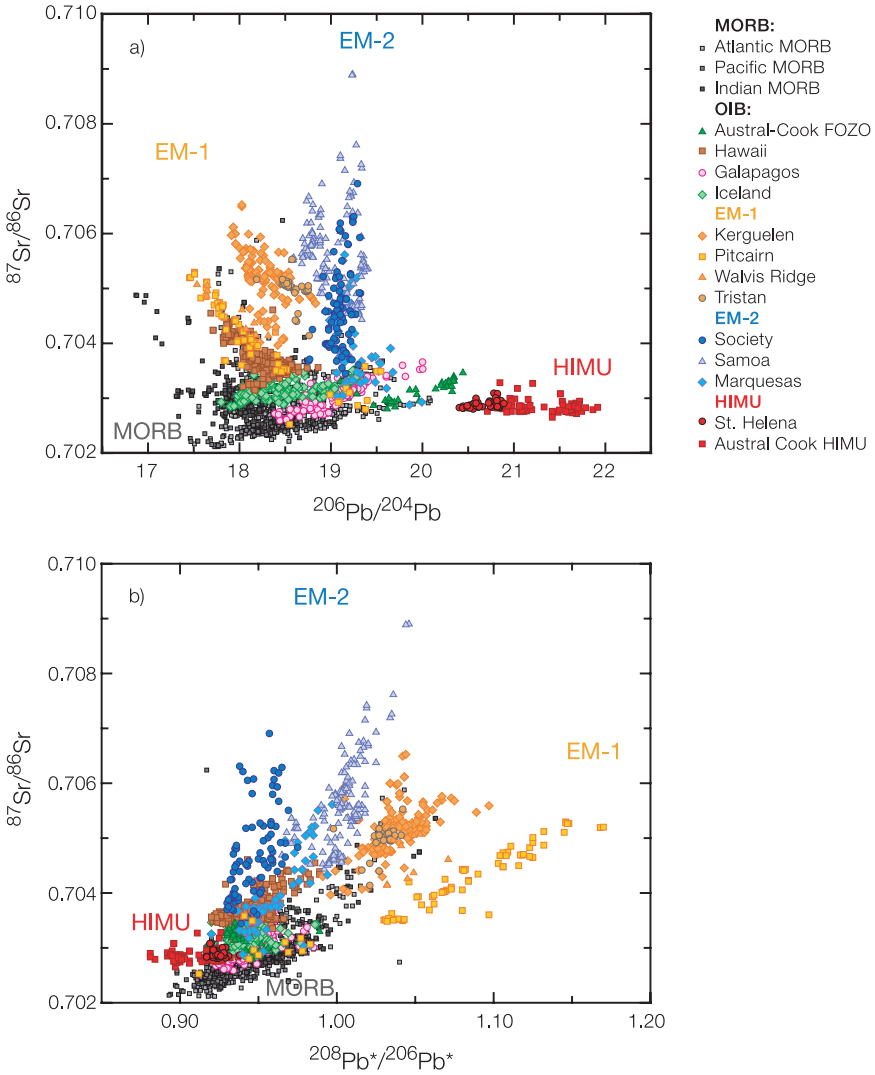

Figure 1. Data for oceanic basalts in (a) $^{87}Sr/^{86}Sr$ versus $^{206}Pb/^{204}Pb$ and (b) $^{87}Sr/^{86}Sr$ versus $^{208}Pb^*/^{206}Pb^*$ space (see *Allègre et al.* [1986] for definition of $^{208}Pb^*/^{206}Pb^*$). HIMU basalts have high $^{206}Pb/^{204}Pb$, low $^{208}Pb^*/^{206}Pb^*$, and low $^{87}Sr/^{86}Sr$, whereas EM-1 basalts have low $^{206}Pb/^{204}Pb$, high $^{208}Pb^*/^{206}Pb^*$, and intermediate $^{87}Sr/^{86}Sr$. EM-2 basalts have intermediate $^{206}Pb/^{204}Pb$, intermediate $^{208}Pb^*/^{206}Pb^*$, and high $^{87}Sr/^{86}Sr$. Data from the compilation of *Stracke et al.* [2003a].

alteration. Nb/Rb ratios, for example, vary from island to island, but the total range in Nb/Rb within one individual sample suite is small (<20%; Figure 2). Similarly, the average Nb/U ratio of all samples is 44.8 ± 8.6 and thereby close to the canonical value of 47 [*Hofmann et al.*, 1986]. This indicates that low-temperature alteration is relatively insignificant for all the samples that passed our tests.

3. Trace Element Ratios as Tracers of Source Composition

[6] In addition to fractional crystallization and alteration, different extents of partial melting (F) may obscure the mantle source characteristics inferred from the chemical composition of OIB. Since La is highly enriched in the melt over Sm (about three to eight-fold at $F = 0.10$ to 0.01), La/Sm ratios are a sensitive indicator for the degree of partial melting. The uniformity of the La/Sm ratios (Figure 3) in OIB from different islands therefore indicates that all samples considered here must have undergone similar degrees of partial melting and derive from sources with similar La/Sm ratios.

[7] Incompatible trace element ratios in erupted melts do, however, only coincide with those in their source in case (1) both elements are either perfectly incompatible (i.e., bulk partition coeffi-

Table 1 (Representative Sample). Major and Trace Element Data for Samples From St. Helena, Gough, and Tristan da Cunha[a] [The full Table 1 is available in the HTML version of this article at http://www.g-cubed.org.]

Sample	H 8	H 13	H 28	H 38	H 64	H 68	H 69	H 74	H 75	H 86
Name	Basanite	Picrobasalt	Basanite	Picrobasalt	Picrobasalt	Picrobasalt	Basalt	Basalt	Basanite	Trachybasalt
SiO_2	44.9	44.2	45.5	43.4	44.3	43.9	45.2	45.0	43.7	46.8
Al_2O_3	17.2	11.3	15.1	9.42	12.6	11.1	13.9	15.1	14.3	15.6
FeO tot	10.5	11.7	12.5	11.1	11.4	11.6	11.3	12.0	11.8	11.8
Fe_2O_3	1.75	1.96	2.09	1.85	1.90	1.93	1.88	2.00	1.97	1.96
FeO [b]	8.93	9.97	10.7	9.45	9.71	9.82	9.61	10.2	10.0	10.0
MnO	0.160	0.170	0.190	0.170	0.170	0.180	0.170	0.180	0.190	0.190
MgO	4.43	13.5	6.64	15.9	11.0	14.3	9.09	6.57	7.81	5.61
CaO	9.81	10.78	9.37	12.7	12.55	10.78	10.93	9.88	10.19	9.2
Na_2O	3.49	1.73	3.89	1.16	2.08	1.68	2.26	2.94	2.21	3.76
K_2O	1.31	0.72	1.25	0.44	0.74	0.67	0.85	1.12	1.03	1.36
TiO_2	3.16	2.29	3.22	1.92	2.6	2.27	2.6	3.28	3.05	2.82
P_2O_5	0.760	0.380	0.690	0.220	0.380	0.340	0.440	0.570	0.550	0.690
LOI	2.62	2.00	0.13	2.88	0.72	1.84	2.10	1.83	3.38	0.70
Mg# [c]	47	71	53	75	67	72	63	53	58	50
Rb	24.9	11.7	24.1	9.81	15.6	13.9	17.4	22.3	18.8	28.1
Sr	892	427	742	327	468	397	526	619	587	684
Y	31.8	21.8	31.6	18.4	25.3	22.1	26.4	30.7	29.4	31.6
Zr	292	183	297	130	197	180	219	267	261	314
Nb	65.6	38.3	66.3	24.9	39.6	37.0	44.5	56.9	57.9	69.5
Cs	0.340	0.275	0.386	0.212	0.142	0.090	0.146	0.168	0.123	0.203
Ba	363	206	359	130	208	183	237	326	313	375
La	46.8	27.2	44.4	17.7	27.4	24.6	30.1	40.8	40.1	47.1
Ce	101	58.2	97.7	39.9	61.8	55.2	66.3	87.0	85.5	100
Pr	11.9	7.06	11.7	4.96	7.55	6.70	8.01	10.3	10.1	11.6
Nd	47.5	29.0	47.6	21.0	31.6	28.0	33.5	41.9	40.8	46.2
Sm	9.12	5.98	9.28	4.55	6.67	5.84	6.92	8.41	8.13	8.83
Eu	2.93	1.91	2.94	1.46	2.17	1.95	2.26	2.75	2.54	2.82
Gd	8.13	5.59	8.34	4.38	6.30	5.61	6.49	7.91	7.26	7.93
Tb	1.10	0.780	1.12	0.610	0.873	0.780	0.900	1.08	1.00	1.08
Dy	5.82	4.21	6.02	3.35	4.82	4.34	4.98	5.91	5.36	5.84
Ho	1.10	0.808	1.15	0.660	0.926	0.838	0.963	1.16	1.04	1.14
Er	2.75	2.00	2.81	1.63	2.31	2.09	2.44	2.82	2.59	2.89
Tm	0.361	0.258	0.366	0.218	0.302	0.267	0.320	0.361	0.337	0.388
Yb	2.26	1.60	2.29	1.38	1.91	1.70	2.06	2.28	2.17	2.46
Lu	0.298	0.207	0.294	0.178	0.247	0.220	0.266	0.300	0.286	0.320
Hf	6.15	4.15	6.39	3.15	4.60	4.11	4.91	5.80	5.64	6.57
Ta	3.93	2.28	3.94	1.49	2.43	2.30	2.75	3.48	3.49	4.23
W	0.9	0.5	0.6	0.1	0.4	0.2	0.3	0.7	0.4	0.6
Pb	2.76	1.66	2.90	0.99	1.52	1.38	1.84	2.48	2.51	3.26
Th	4.81	2.96	4.56	1.82	2.82	2.49	3.21	4.25	4.36	5.15
U	1.61	0.77	1.33	0.52	0.82	0.75	0.94	1.19	1.18	1.45
Sc [d]	18	38	25	46	45	38	34	25	29	27
V	160	241	199	205	246	208	210	229	231	208
Cr	36	735	166	878	514	795	336	146	224	157
Co	27	72	42	60	52	57	42	38	42	41
Ni	26	316	97	369	221	289	150	76	97	80

[a] Major element data are in % wt. Trace element data are in μg/g. The letter in the sample name indicates the island from which the sample was obtained: H, St. Helena; G and B, Gough; T, Tristan da Cunha.

[b] Assuming $Fe^{2+}/Fe^{3+} = 0.85$.

[c] $Mg\# = (Mg^{2+}/(Mg^{2+}+Fe^{2+})) \times 100$.

[d] Concentrations of Sc, V, Cr, Co, and Ni determined using ^{43}Ca as internal standard for LA-ICPMS.

[e] For the purpose of this paper, the official registration numbers of the Tristan samples supplied by the Natural History Museum, London have been simplified so that the samples with the original registration number BM 1962, 128 (1) at the Natural history Museum is simply referred to as T 1 in this study.

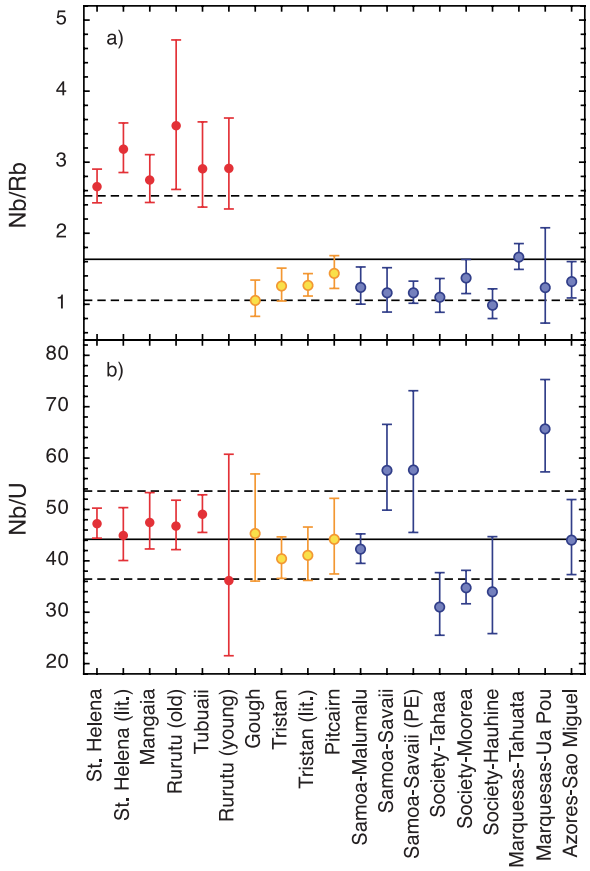

Figure 2. Averages and variations (1σ) of (a) Nb/Rb and (b) Nb/U ratios for individual ocean islands. Although the absolute Nb/Rb ratios are different from island to island, the variation within each suite is generally less than 20% (except for older series samples from Rurutu and Marquesas-Ua Pou), documenting the freshness of all samples. The average of the Nb/U ratio of all islands is close to the "canonical" value of 47 for oceanic basalts [*Hofmann et al.*, 1986]. Note that due to the logarithmic distribution of very incompatible element concentrations in terrestrial rocks [*Ahrens*, 1954] all averages and standard deviations have been calculated from logarithmic values in order to obtain a normal distribution of the data sets and were converted back to a linear scale.

cient D = 0), (2) their bulk partition coefficient is much smaller than the melt fraction (D ≪ F), or (3) both elements are similarly incompatible. For most of the elements and element ratios used in the following to compare mantle sources, either D → 0 or D ≪ F, or both, appear to be reasonable assumptions.

[8] *Sims and DePaolo* [1997] have shown that the relative compatibility difference between two elements is best evaluated by using plots of log (A) versus log (B), with A and B being the concentrations of two different trace elements (Figure 4). In this space, only element pairs with identical incompatibility form linear trends with a slope of unity [*Sims and DePaolo*, 1997]. Differences in D values of the two elements A and B result in a nonlinear array (for a comprehensive treatment of this topic, see *Sims and DePaolo* [1997]). However, the associated statistical and analytical errors are often too large to resolve the small deviations from linearity between the most incompatible elements (Rb, Ba, Th, U, Nb, Ta, K, La). As a consequence, using a linear fit might provide a reasonable first *approximation* of the relative compatibility contrast between two elements [*Hofmann*, 2004]. Figure 4 shows examples for some of the element ratios for which similar incompatibility can be asserted with a reasonable degree of confidence, inferred from both a nonlinear regression similar to *Sims and*

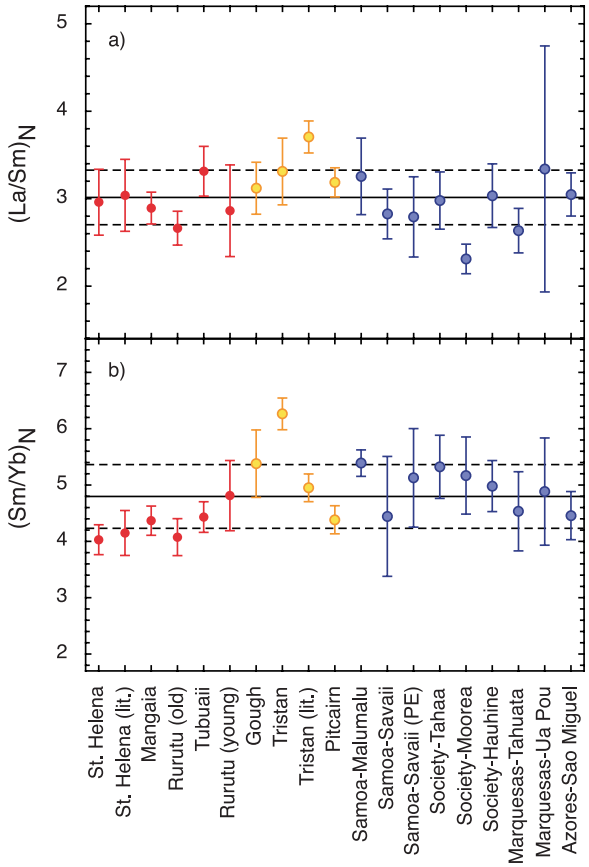

Figure 3. Averages and variations (1σ) of CI chondrite normalized (a) La/Sm ratios and (b) Sm/Yb ratios for individual islands. All suites have comparable and high La/Sm_N (2.99 ± 0.3) and Sm/Yb_N ratios (4.79 ± 0.56), indicating that all OIB have been produced by similar degrees of partial melting in the garnet-stability field. Normalizing values are from *Anders and Grevesse* [1989].

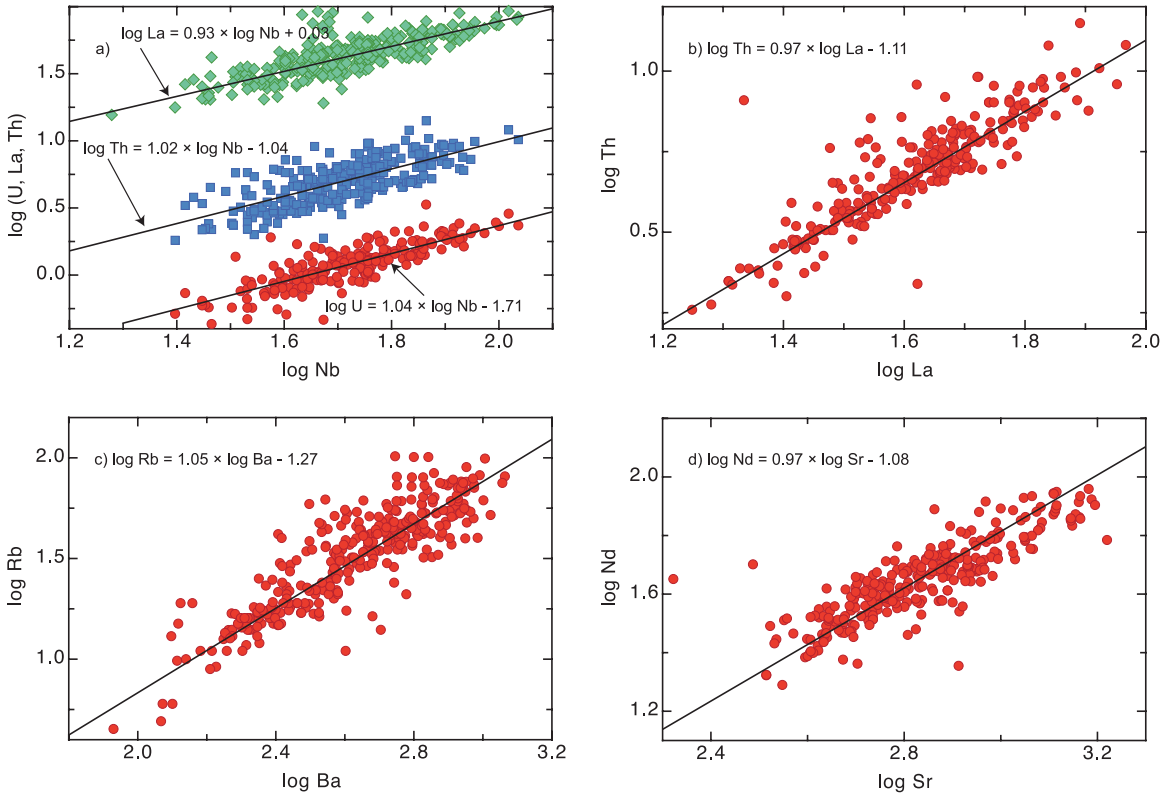

Figure 4. Concentrations of (a) Nb versus U, La, and Th, (b) La versus Th, (c) Ba versus Rb, and (d) Sr versus Nd. In these logarithmic plots, element pairs of similar incompatibility form linear trends with a slope close to unity. See text for further explanation and *Sims and DePaolo* [1997] for comprehensive discussion of the mathematical background.

DePaolo [1997] and the linear regression presented in Figure 4.

4. Trace Element Characteristics of OIB and Their Sources

4.1. Characteristics Common to All OIB

[9] All OIB investigated in this study have subparallel rare earth element (REE) patterns showing enrichment in light REE (LREE) relative to average CI chondrite and primitive upper mantle (PUM) (Figure 5). All samples are depleted in heavy REE (HREE) relative to middle REE and LREE concentrations suggesting that melting occurred mainly in the garnet stability field (see also Figure 3). The ratios between the alkali and alkaline earth elements (e.g., Rb/K, Ba/K) and the La/Th and Sr/Nd ratios are similar in all OIB, with the exception of some samples from Marquesas-Ua Pou (see Figure 6; (Rb/K) × 10000 = 27.4 ± 6.5, (Ba/K) × 10000 = 365 ± 96, La/Th = 8.6 ± 1.4 and Sr/Nd = 0.067 ± 0.015). Similar (Ba, Rb)/K ratios might be due to buffering of Rb, Ba, and K by residual hydrous phases such as phlogopite or amphibole during partial melting [e.g., *Hart*, 1988; *Sun and McDonough*, 1989]. Amphibole, however, is not stable in the source regions of OIB (garnet-stability field >2–2.5 GPa), and the presence of phlogopite would raise the bulk $D_{Rb, Ba, K}$ to values that are no longer considerably smaller than the degree of partial melting (see above). This would lead to considerable variability in the ratios of alkali and alkaline earth elements and other incompatible elements (e.g., Nb). The small spread in Rb/Nb ratios (Figure 2a) therefore indicates that phlogopite is not *generally* present in the source regions of OIB.

[10] The relatively uniform Sr/Nd ratios (Figure 6d) are expected from the linear mixing trends in Sr-Nd isotope space [see, e.g., *Hart*, 1988], the apparent similar compatibility of Sr and Nd during OIB melting (Figure 4), and the often minor role of plagioclase fractionation during fractional crystallization of alkaline basalts (at least for samples containing more than 5% MgO [*Sack et al.*, 1987]), and show that the OIB suites investigated here likely originate from sources with similar Sr/Nd ratios.

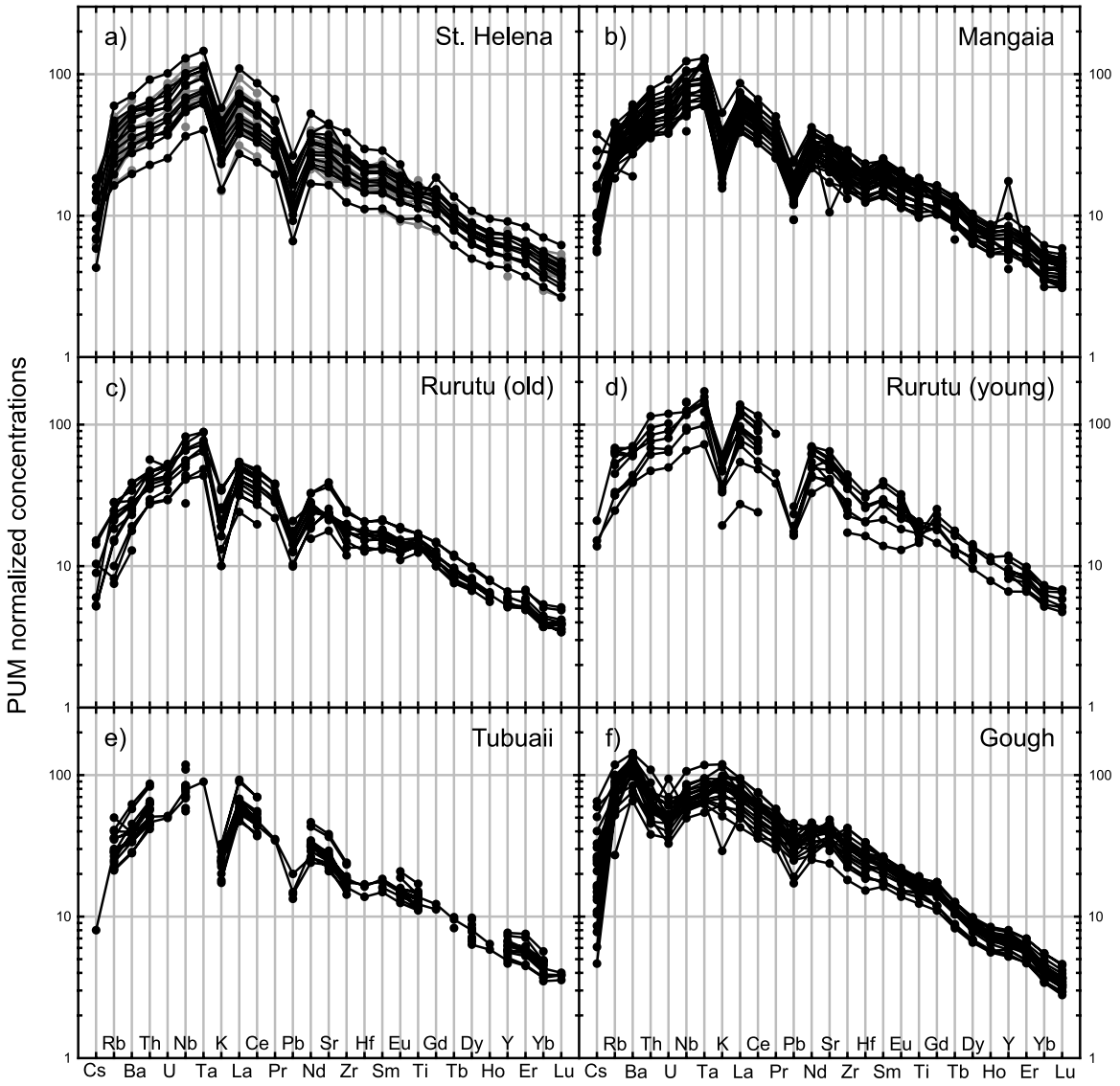

Figure 5. Primitive upper mantle (PUM) [*McDonough and Sun*, 1995] normalized trace element patterns of investigated sample suites. Note that enrichment of Nb and Ta and depletion of Pb are common features of all suites. (a to e) HIMU basalts are strongly depleted in very incompatible elements, whereas (f to r) EM basalts are less depleted but more heterogeneous with respect to the very incompatible element abundance. Gray symbols in Figures 5a and 5g refer to data from the literature (see auxiliary material).

[11] The relatively uniform La/Th ratios (Figure 6c) show that although ratios of very incompatible elements (Cs, Rb, Ba, Th, U, Nb, Ta, K) and LREE ratios in general can be highly variable, La and Th represent a common anchor for LREE-very incompatible element depletion/enrichment patterns in OIB sources.

4.2. HIMU Basalts

[12] Our new data compilation shows that HIMU basalts from different localities have remarkably similar trace element compositions (Figures 5a to 5e). All HIMU basalts are enriched in Nb and Ta relative to Ba and Rb (Figure 7a) and are overall depleted in Pb, Rb and Ba relative to EM basalts (Figures 8a and 8b). HIMU basalts also have the lowest Rb/Sr ratios of all OIB (Figure 8c). Although Rb and Sr are likely to be fractionated during partial melting, the Rb/Sr ratios in HIMU basalts are remarkably similar over a wide range of Sr concentrations. In combination with their relatively constant $^{87}Sr/^{86}Sr$ ratios (Figure 1) this implies that all HIMU sources have similarly low Rb/Sr ratios.

[13] The decrease in normalized concentrations from Nb to Cs is a unique feature of HIMU basalts

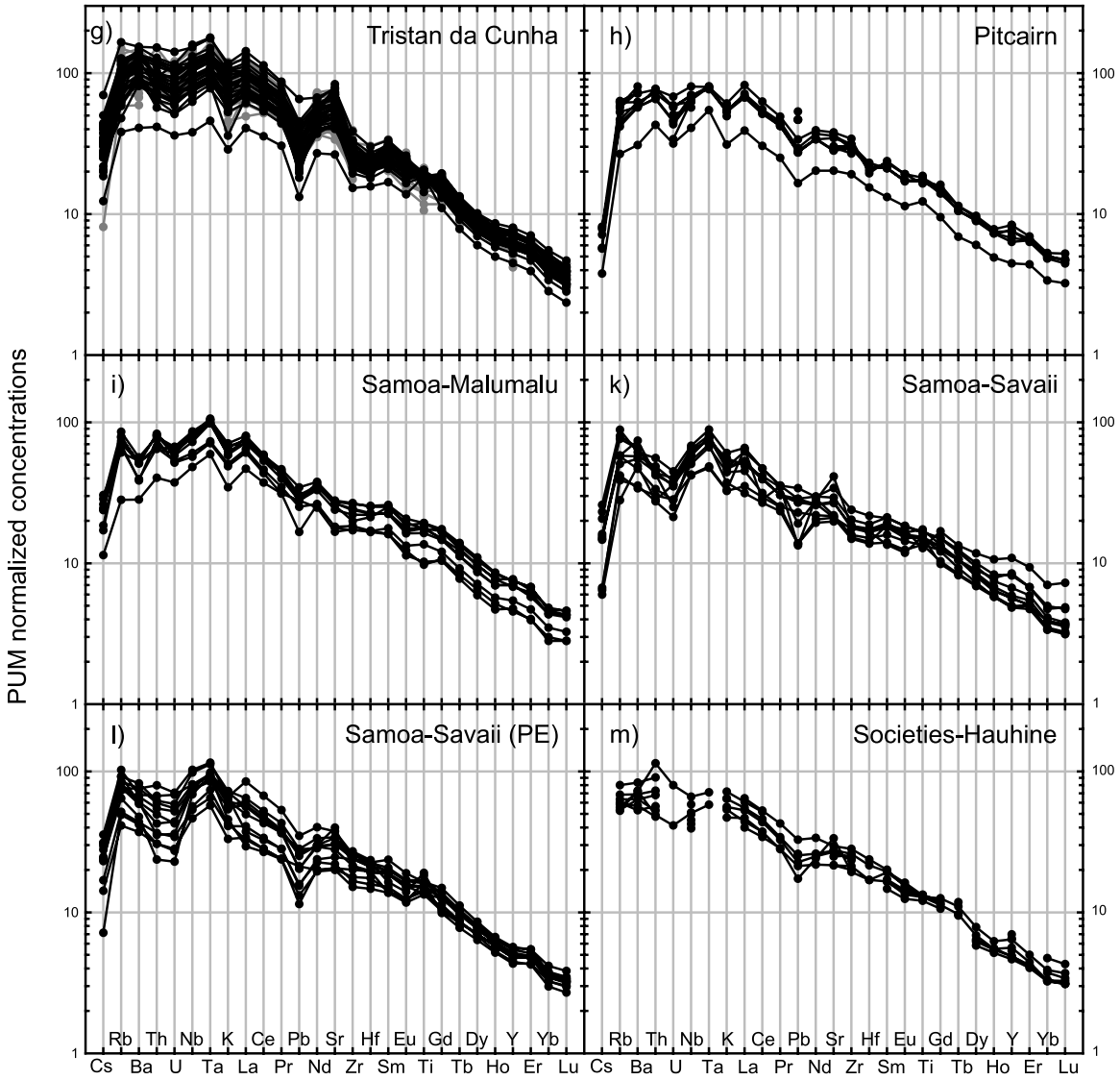

Figure 5. (continued)

that distinguishes them from all EM basalts (Figures 5f to 5r). Figure 9 shows the calculated trace element abundances in the source of St. Helena basalts. Calculations are done using accumulated nonmodal fractional melting [*Shaw*, 1970] of a garnet-peridotite source with four different sets of partition coefficients and modal compositions [*Kelemen et al.*, 2003; *Stracke et al.*, 2003a; *Salters and Stracke*, 2004; *Workman et al.*, 2004], and a range of different degrees of partial melting (0.5–5%). Despite the remaining uncertainties in the input parameters and the fact that such simple models are likely to be an oversimplification of the actual melting process, some general inferences about the composition of the HIMU sources are possible: The HIMU source is characterized by (Rb, Ba, Th, U)/REE and Rb/Sr ratios lower than, and by (U, Th)/Pb, Sm/Nd, and (Nb, Ta)/La ratios higher than those in Bulk Earth. These conclusions are consistent with the low Ba/La, Rb/La, Rb/Sr (Figures 8 and 10), and high U/Pb ratios (Figure 11) and the Sr-Nd-Pb isotope systematics in HIMU basalts ($^{87}Sr/^{86}Sr$ lower than and $^{143}Nd/^{144}Nd$ higher than Bulk Earth, and the most radiogenic Pb isotope ratios in all OIB; Figure 1).

4.3. EM Basalts

[14] EM basalts are characterized by highly variable trace element ratios, both within and between samples from individual localities. Probably the most conspicuous general feature that distinguishes all EM basalts from HIMU basalts is the consistently high Th/U ratios in EM compared to HIMU

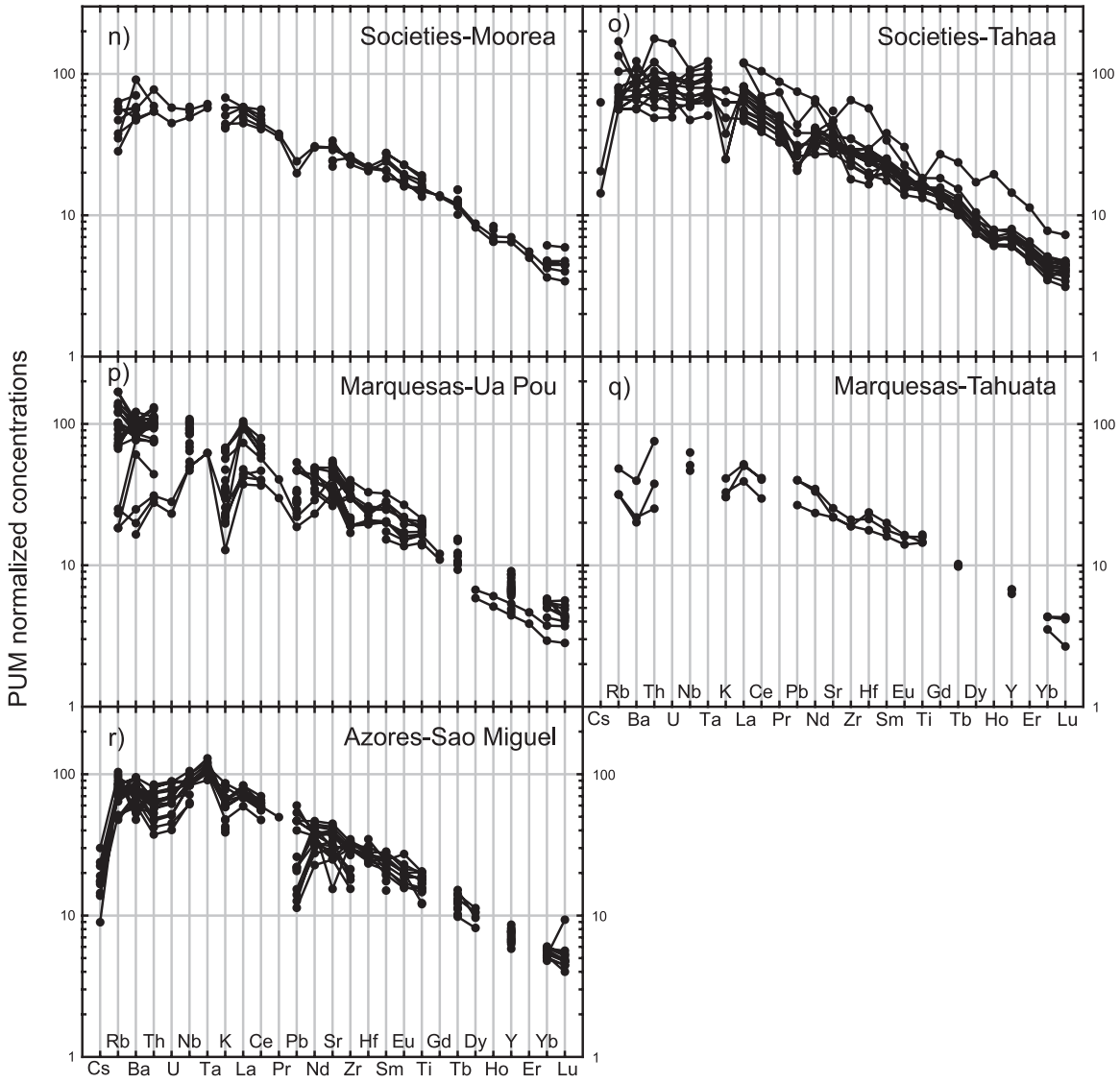

Figure 5. (continued)

basalts (Figure 11f). Sao Miguel, however, is exceptional, since the Sao Miguel basalts are the only EM basalts with low Th/U ratios similar to those in HIMU basalts. As shown earlier, the La/Th and La/Sm ratios are relatively constant in all OIB investigated here (Figures 3 and 6). This suggests that trace element ratios with La as the reference element are well suited to show the relative enrichments and depletions of incompatible trace elements in different OIB suites (Figures 10 and 11).

[15] (Rb, Ba, K)/La ratios are higher in EM than in HIMU basalts (Figure 10). The fact that both Rb/Nb and Rb/La (Figures 7 and 8) and $^{87}Sr/^{86}Sr$ ratios are consistently higher in EM basalts compared to HIMU basalts suggests that Rb is enriched in EM compared to HIMU basalts and their sources. Similar arguments for enrichment of Ba and K in EM basalts can be made but some EM basalts also have, on average, lower Ba/La and K/La ratios than HIMU basalts (Samoa-Malumalu, Marqueses-Tahuata and Ua Pou). The lower Nb/La (Figure 10e) and Nb/Th ratios (not shown) in EM relative to HIMU basalts further indicate that EM basalts are less enriched in Nb (Ta) than HIMU basalts. The Savaii posterosional samples with their high Nb/La and Nb/Th ratios, which are due to low Th and REE concentrations (Figure 7) are an exception [see also *Workman et al.*, 2004, Figures 11 and 12]. Similar observations are made on the basis of the calculated source concentrations of four different EM-type localities (Gough, Pitcairn, Samoa-Malumalu, and Society-Tahaa; Figure 12; for details of the calculations, see Figure 9). In summary, therefore,

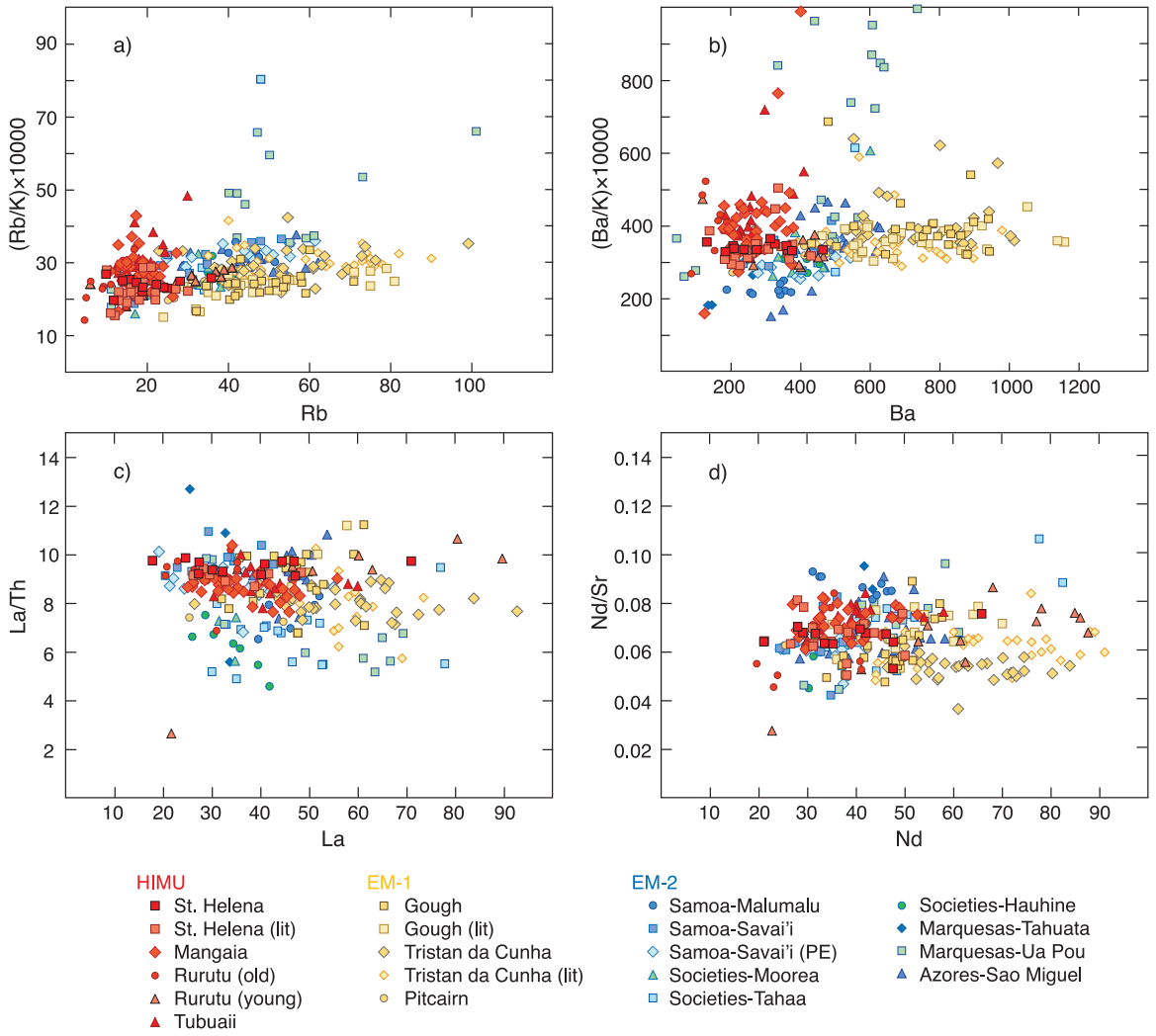

Figure 6. Data of ocean island basalts in (a) Rb/K versus Rb, (b) Ba/K versus Ba, (c) La/Th versus La, and (d) Nd/Sr versus Nd space. Rb/K, Ba/K, La/Th, and Nd/Sr ratios are rather uniform and do not vary with absolute concentrations (except some samples from Marquesas-Ua Pou).

EM basalts and their corresponding sources are enriched in Rb, Ba, and K and depleted in Nb and Ta, and have higher Th/U ratios compared to HIMU basalts. The relative abundances of very incompatible elements for different EM sources, however, do not follow a coherent pattern (see discussion below). Note that the calculated source concentrations of both HIMU and EM basalts are elevated compared to Bulk Earth (Figures 9 and 12), but that the LREE and very incompatible element concentrations (Cs to La) are generally depleted relative to the HREE concentrations.

[16] The variations in Th/La, Rb/La, Ba/La, Th/U, Nb/Th, K/La, and Ba/Nb ratios in basalts from four of the isotopically most extreme EM-1 and EM-2 localities (Pitcairn and Gough for EM-1, and Samoa-Malumalu and Society-Tahaa for EM-2; Figure 13) show no systematic enrichment or depletion of individual incompatible elements or ratios thereof that clearly distinguish EM-1 and EM-2 sources. Especially Ba/Nb ratios have often been used to discriminate between EM-1 and EM-2 basalts. *Weaver* [1991] has argued that high Ba abundances (high Ba/Nb, Ba/Th, Ba/La ratios) are typical for EM-1 and that high Th/Nb and Th/La ratios are typical for EM-2 basalts. With the more comprehensive data set used here, systematic differences between the Th/La, Th/Nb, and especially the Ba/Nb ratios in EM-1 and EM-2 basalts cannot be confirmed. Samples from Gough (EM-1) and Society-Tahaa (EM-2) have the highest, and samples from Pitcairn (EM-1) and Samoa-Malumalu (EM-2) have the lowest Ba/Nb ratios, respectively (Figure 13). Thus Ba/Nb ratios covering the entire

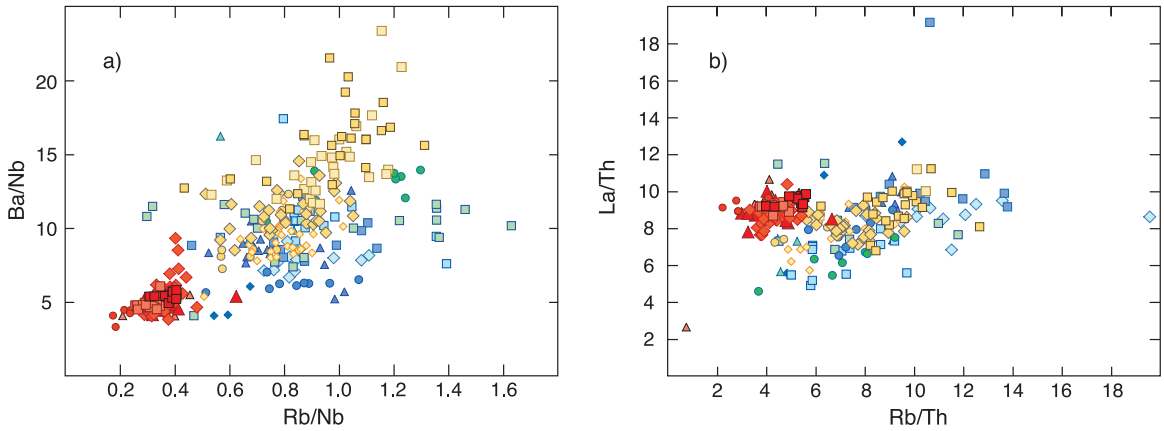

Figure 7. Data of ocean island basalts in (a) Ba/Nb versus Rb/Nb and (b) La/Th versus Rb/Th space. HIMU basalts have relatively uniform Ba-Rb-Nb and Rb-La-Th systematics, suggesting that their sources have rather uniform very incompatible element compositions. Ba/Nb and Rb/Nb ratios are lower in HIMU basalts than in EM basalts indicating that the sources of HIMU basalts are enriched in Nb (Ta) relative to other very incompatible elements. Symbols as in Figure 6.

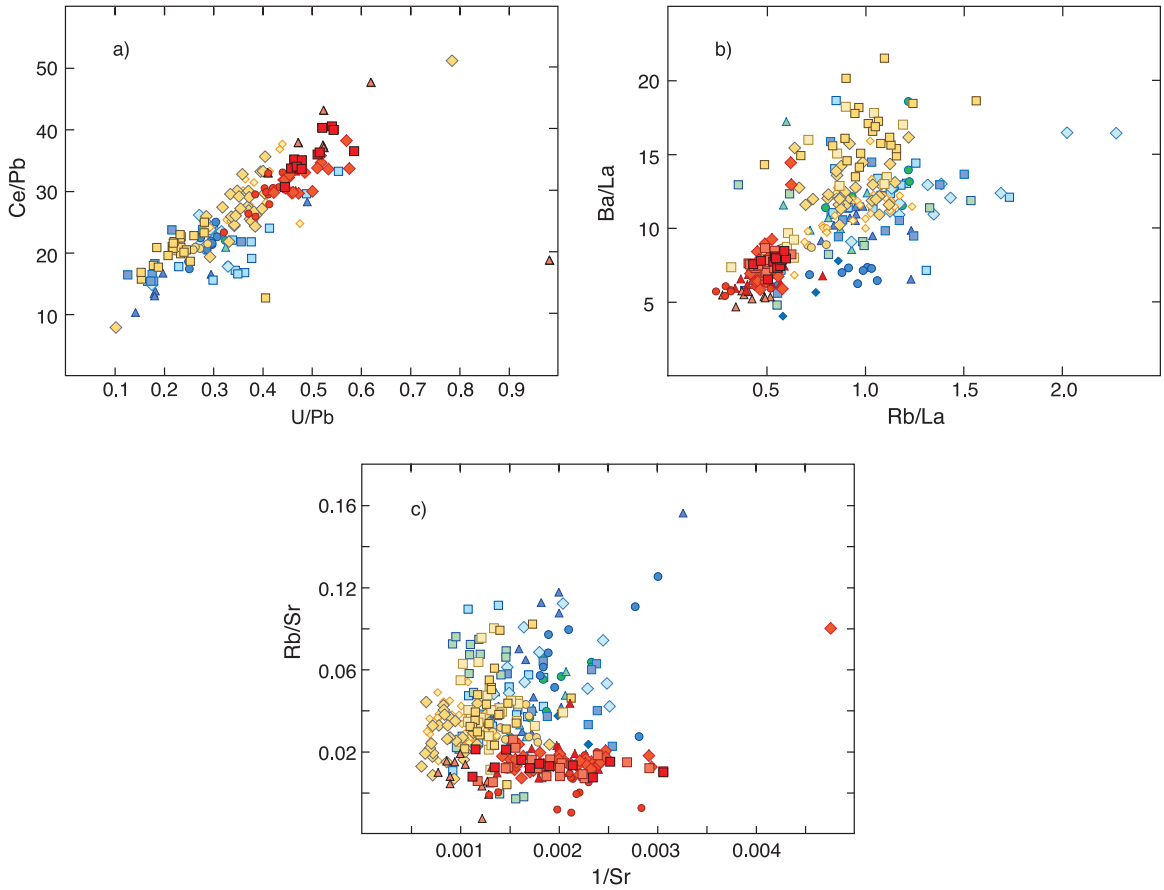

Figure 8. Data of ocean island basalts in (a) Ce/Pb versus U/Pb, (b) Ba/La versus Rb/La, and (c) Rb/Sr versus 1/Sr space. High Ce/Pb and U/Pb and low Ba/La and Rb/La ratios indicate that HIMU basalts are more depleted in Pb, Ba, and Rb than EM basalts. HIMU basalts have uniform and consistently lower Rb/Sr ratios than in EM basalts. Symbols as in Figure 6.

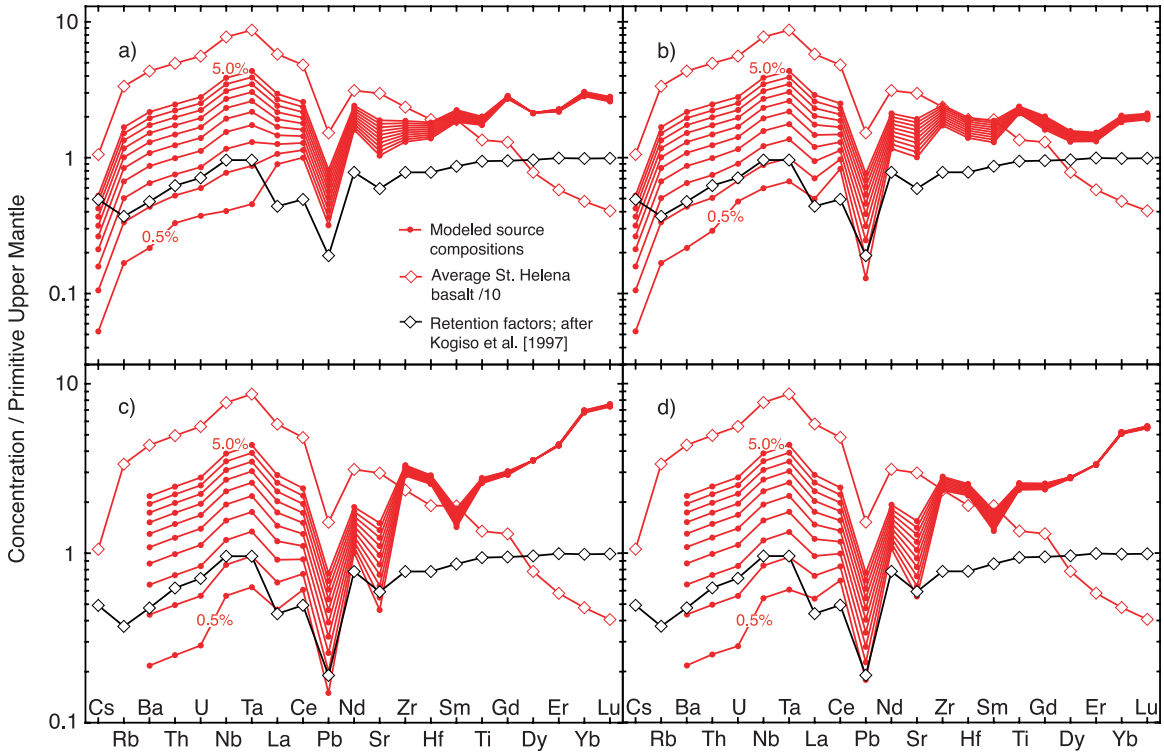

Figure 9. Calculated PUM-normalized trace element patterns of the St. Helena source assuming accumulated nonmodal fractional melting [*Shaw*, 1970] of a garnet-peridotite source for a range of different degrees of partial melting and bulk partition coefficients from (a) *Stracke et al.* [2003a], source mode Ol:Opx:Cpx:Grt = 0.55:0.25:0.12:0.08, melting mode Ol:Opx:Cpx:Grt = 0.05:0.05:0.45:0.45; (b) *Salters and Stracke* [2004], source mode = 0.53:0.08:0.34:0.05, melting mode = −0.05:0.49:−1.31:−0.13; (c) *Kelemen et al.* [1992, 2003], source mode = 0.54:0.17:0.09:0.20, melting mode = 0.10:0.18:0.30:0.42; and (d) *Workman et al.* [2004], assuming same partition coefficients and garnet-peridotite modal compositions as *Kelemen et al.* [2003] but weighted to 72% garnet peridotite and 28% spinel peridotite (source mode Ol:Opx:Cpx:Sp = 0.46:0.28:0.18:0.08, melting mode Ol:Opx:Cpx:Sp = 0.45:0.55:0.67:0.22). Arrays of curves show different degrees of melting (F = 0.5 to 5% using increments of 0.5%). The normalized concentrations of average St. Helena basalt have been divided by 10. Also shown are the mobility coefficients in a fluid-rock system [*Kogiso et al.*, 1997]. Note that the plotted coefficients are converted to "retention" factors (=1-mobility coefficient) and reflect the fraction retained in the source. Although the modal compositions and the absolute values for the bulk partition coefficients differ, the depletion in very incompatible elements and light REE relative to heavy REE, the enrichment of Nb and Ta relative to U and La, and the depletions in Pb relative to Nd are common to all modeled source compositions and are difficult to reconcile with partial melting processes alone. Comparison with rock-fluid alteration factors suggests that the HIMU source must have experienced fluid-rock interaction during its evolution.

spectrum are observed in both EM-1 and EM-2 basalts. Similar observations are made if this type of analysis is extended to other trace element ratios. As a consequence, EM basalts cannot be grouped into EM-1 and EM-2 on the basis of their trace element concentrations, nor can any other grouping be identified.

[17] As a family, therefore, EM basalts have common trace element characteristics that distinguish them from HIMU, but each suite of EM basalts has its own unique very incompatible trace element signature that is different from those of any other suite of EM basalts and is ultimately related to a unique source composition.

5. Implications for the Origin of OIB Sources

5.1. Nature of the HIMU Source

[18] The apparent depletion of the very incompatible elements (Cs to U) relative to the REE and the enrichment of most other trace elements with respect to Bulk Earth (Figure 9) in the inferred HIMU source suggests that HIMU basalts are most

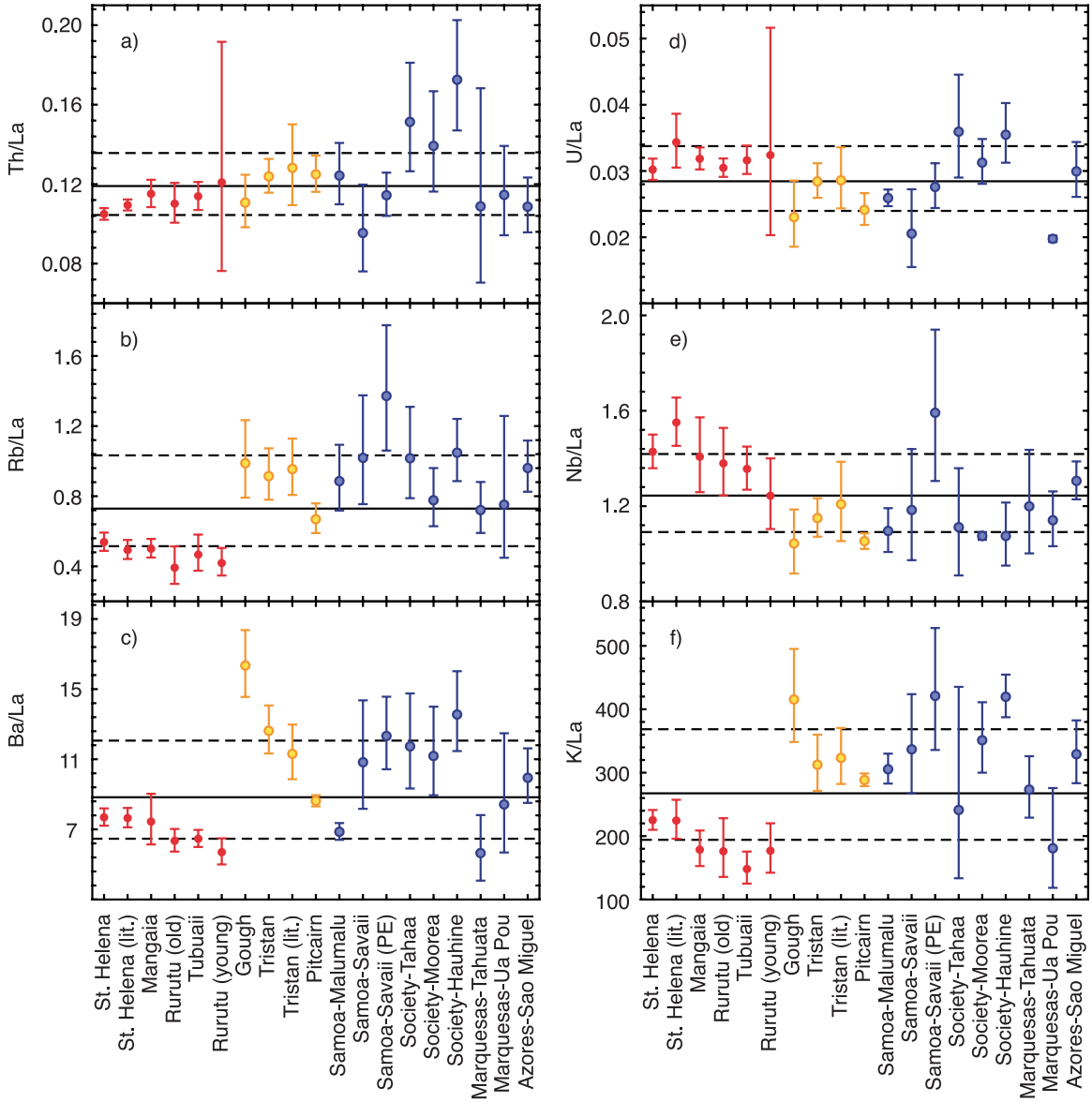

Figure 10. Averages and variations (1σ) of ratios of very incompatible elements and La for individual island suites. Note that HIMU basalts (St. Helena, Mangaia, Rurutu (old/young), and Tubuaii, red symbols) are distinct with respect to most ratios relative to EM basalts (except Th/La). Each EM basalt suite has a unique trace element signature that is different than those of any other suite and thus does not allow unambiguous discrimination between EM-1 (Gough, Tristan, Pitcairn, yellow symbols) and EM-2 basalts (all others, blue symbols).

likely produced by melting of very incompatible element and LREE depleted precursors. Mid-ocean ridge basalts (MORB) display a large compositional variety [*Hofmann*, 2004], but melting of the depleted mantle is the only known process that yields large volumes of incompatible element enriched (with respect to Bulk Earth), but very incompatible element and LREE depleted rocks (i.e., MORB). Subducted oceanic lithosphere (basaltic crust plus oceanic lithospheric mantle) therefore appears to be a suitable candidate for HIMU sources.

[19] Some of the observed trace element fractionations in HIMU basalts and their calculated sources, however, are difficult to produce by partial melting processes alone, i.e., the generation and remelting of recycled oceanic lithosphere. The similar bulk partition coefficient ratios of Nb, Ta and U (Figure 4) and the small range of Nb/U ratios in oceanic basalts (Figure 2) [*Hofmann et al.*, 1986; *Sims and DePaolo*, 1997; *Hofmann*, 2004] indicate that Nb and Ta are hardly fractionated from neighboring elements (e.g., U, La) during partial melting. Thus the enrichment of Nb and Ta relative to neighboring

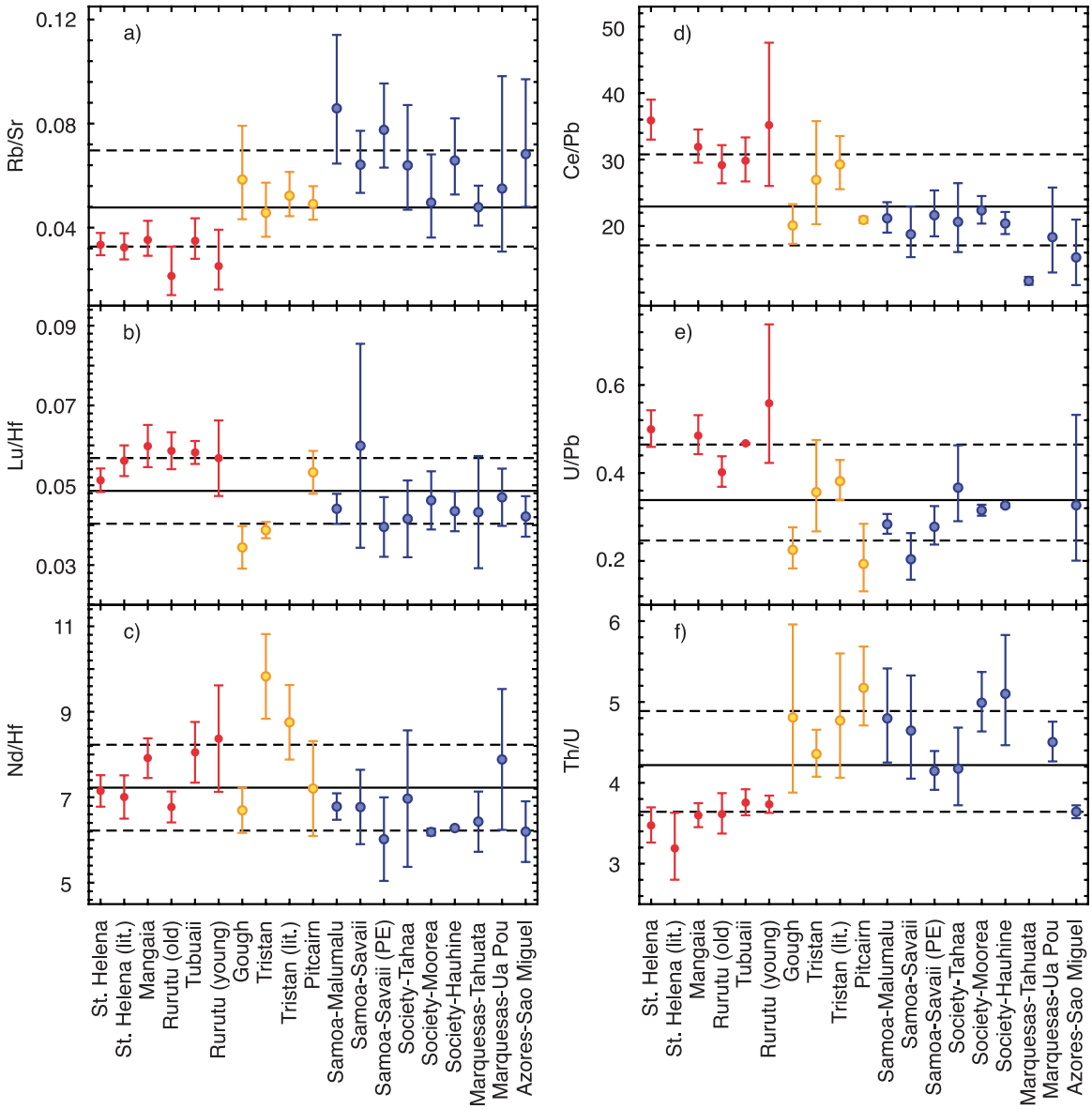

Figure 11. Averages and variations (1σ) of parent/daughter ratios of the Sr, Pb, and Hf isotope decay systems as well as Ce/Pb, Th/U, and Nd/Hf ratios for individual island suites. EM basalts have generally higher Th/U and Rb/Sr and lower Lu/Hf, Nd/Hf, U/Pb, and Ce/Pb ratios compared to HIMU basalts.

elements in HIMU basalts suggests that processes other than partial melting might be involved in the genesis of HIMU sources.

[20] The composition of arc lavas and experimental studies of fluid-rock interaction in subarc environments indicate that dehydration of subducted MORB leads to net loss of Cs, Rb, Ba, K, the LREE, Pb and Sr but relative enrichment of Nb (Ta) due to removal of fluid-mobile elements and/or retention of Nb and Ta in residual rutile [*McCulloch and Gamble*, 1991; *Brenan et al.*, 1994, 1995; *Keppler*, 1996; *Kogiso et al.*, 1997; *Ayers*, 1998; *Stalder et al.*, 1998; *Foley et al.*, 2000; *Klemme et al.*, 2002, 2005]. The extent of mobilization by subduction-zone fluids increases smoothly from U toward Rb. It is significantly higher for Pb and Sr compared to Nd and is significantly lower for Nb and Ta compared to U and La (Figure 9) [*Tatsumi et al.*, 1986; *Kogiso et al.*, 1997; *Tatsumi and Kogiso*, 1997]. Thus, while the absolute abundances of the fluid-mobile elements are changed, fluid-rock interaction preserves the smoothly decreasing incompatible element pattern (U to Cs) of subducted oceanic crust, albeit with slightly different slope.

[21] The inferred characteristics of the HIMU source, i.e., the general enrichment of incompatible

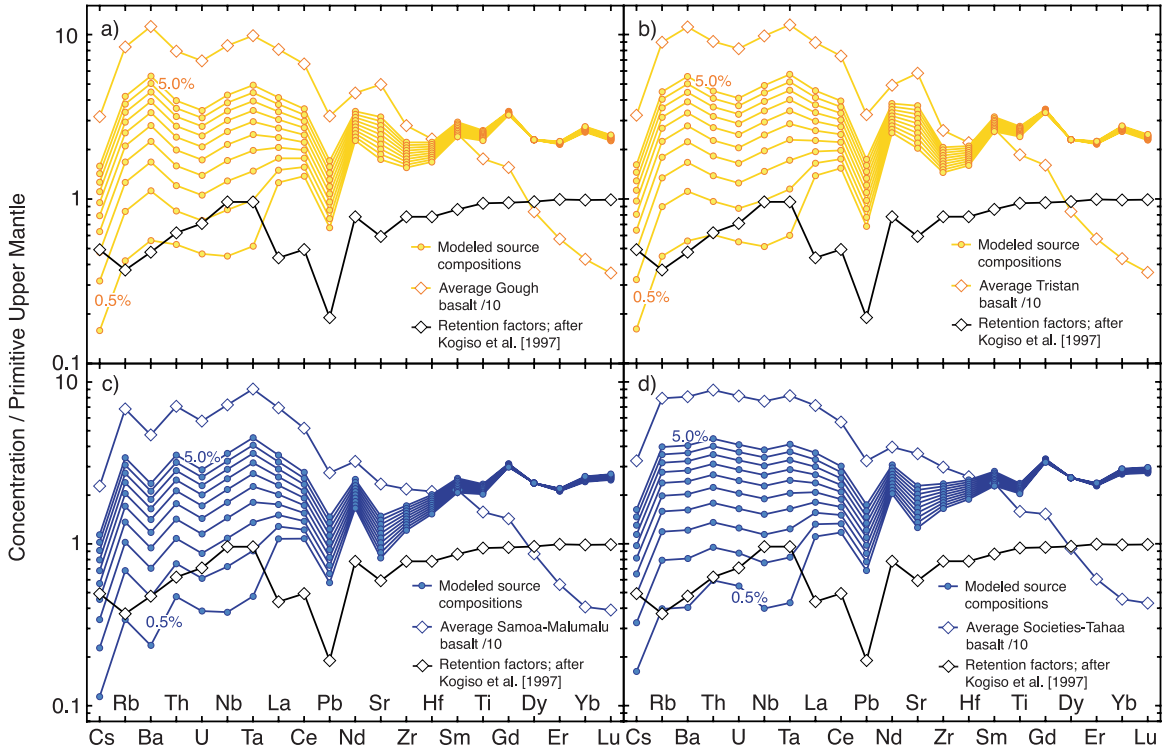

Figure 12. Calculated PUM-normalized trace element patterns of average sources of (a) Gough, (b) Tristan, (c) Samoa-Malumalu, and (d) Societies-Tahaa basalts using the same model parameters as described in the caption of Figure 9. The normalized concentrations of average basalts have been divided by 10. The EM sources show irregular patterns of very incompatible elements and negative spikes for Pb. Similar to the HIMU source (Figure 9), they are depleted in very incompatible elements and light REE relative to heavy REE. Comparison with rock-fluid retention factors suggests that the EM source must have experienced fluid-rock interaction during its evolution. The enriched very incompatible element patterns of the EM sources compared to the HIMU sources require the presence of an additional enriched component.

trace elements in the HIMU source over PUM, the depletion of very incompatible trace elements and LREE relative to the HREE, the enrichment of Nb-Ta relative to U and La, and the depletion of Pb relative to Nd, provide a strong case that HIMU sources were formed by melting of very incompatible element and LREE depleted sources that were subsequently modified by fluid-rock alteration processes in the subarc environment. In other words, the trace element systematics support the notion that HIMU sources represent recycled ancient subduction-modified oceanic lithosphere [*Hofmann and White*, 1982; *Vidal et al.*, 1984; *White*, 1985; *Palacz and Saunders*, 1986; *Zindler and Hart*, 1986; *Halliday et al.*, 1988; *Hart*, 1988; *Nakamura and Tatsumoto*, 1988; *Weaver*, 1991; *Chauvel et al.*, 1992, 1997; *Hauri and Hart*, 1993; *Reisberg et al.*, 1993; *Roy-Barman and Allègre*, 1995; *Hauri et al.*, 1996; *Niu and Batiza*, 1997; *Lassiter and Hauri*, 1998; *Salters and White*, 1998; *Niu et al.*, 1999; *Stracke et al.*, 2003a, 2005; *Hofmann*, 1997, 2004]. In addition, the expected high U/Pb and Th/

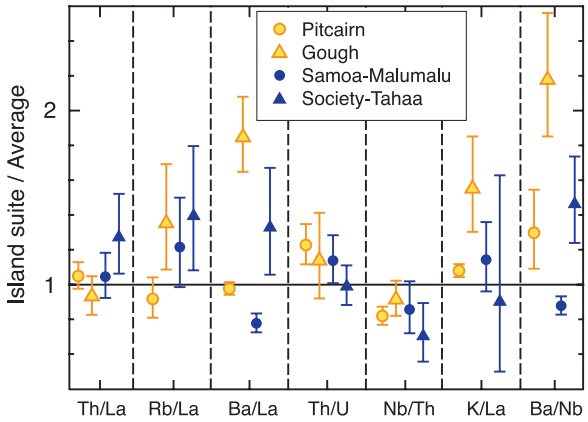

Figure 13. Comparison of trace element ratios of EM-1 basalts (Pitcairn, Gough) and EM-2 basalts (Samoa-Malumalu, Society-Tahaa) normalized to the mean value of all investigated OIB (compare Figures 10 and 11). Also shown are the variations of respective ratios within each suite (1σ). The overlap in variations of the trace element ratios shows that it is difficult to distinguish EM-1 or EM-2 basalts on the basis of their trace element composition. The same observation is made using different trace element ratios.

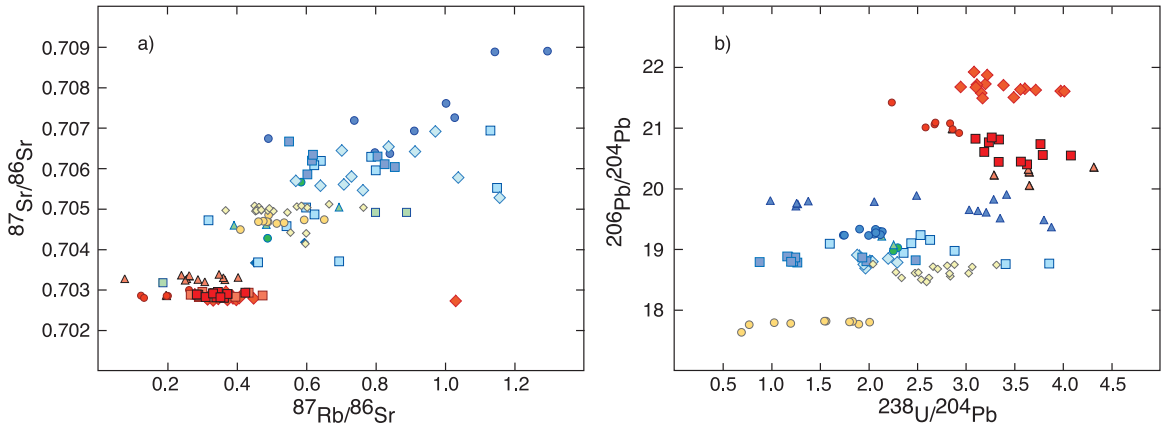

Figure 14. (a) $^{87}Sr/^{86}Sr$ versus $^{87}Rb/^{86}Sr$ and (b) $^{206}Pb/^{204}Pb$ versus $^{238}U/^{204}Pb$ in ocean island basalts. Despite the large variations in parent/daughter ratios in individual sample suites, EM basalts have higher $^{87}Rb/^{86}Sr$ and lower $^{238}U/^{204}Pb$ ratios, consistent with their higher $^{87}Sr/^{86}Sr$ and lower $^{206}Pb/^{204}Pb$ ratios. The positive trends further suggest that variations in $^{87}Sr/^{86}Sr$ and $^{206}Pb/^{204}Pb$ between different OIB are primarily the result of systematic variations of $^{87}Rb/^{86}Sr$ and $^{238}U/^{204}Pb$ ratios of different sources and are to a lesser degree caused by different source ages. Symbols same as in Figure 6.

Pb ratios in the subduction-modified oceanic lithosphere are in good agreement with the radiogenic Pb isotope signatures in HIMU basalts [*Hart and Staudigel*, 1989; *Chauvel et al.*, 1992; *Rehkämper and Hofmann*, 1997; *Stracke et al.*, 2003a; *Kelley et al.*, 2005].

[22] The uniform trace element composition of all HIMU basalts and their corresponding sources in combination with their comparatively small range in isotopic composition further suggests that the HIMU sources must have evolved with remarkably uniform composition for similar time periods, *irrespective* of their inferred genetic origin [see also *Stracke et al.*, 2003a, 2005]. Consequently, it appears most likely that the HIMU sources were formed under similar conditions at roughly the same time; i.e., the HIMU source is likely to represent a real mantle reservoir. The term reservoir is used here for a certain part of the mantle that is compositionally homogeneous and originated from a single process at a given time.

5.2. Nature of the EM Sources and the Trace Element–Isotope Conundrum

[23] In general, the similarities between EM and HIMU (similar La/Sm, Sr/Nd, La/Th, (Rb, Ba)/K and Nd/Hf ratios in all OIB investigated here, the depletion of Pb relative to Ce and Nd, and the LREE depleted pattern of the inferred sources; Figures 3, 5, 6, 7, 11, and 12) suggest that a precursor similar to that of the HIMU source, i.e., subduction-modified oceanic lithosphere, is also involved in the genesis of EM sources. However, Th/U ratios are consistently higher (Figure 11f), Nb and Ta are less enriched (Figure 10e), and the very incompatible elements are more enriched and more variable in EM compared to HIMU sources (Figure 5). Moreover, the Ce/Pb and U/Pb and the $^{206}Pb/^{204}Pb$ ratios are generally lower in EM compared to HIMU basalts (Figures 1, 11d, 11e, and 14) [see also *Sun and McDonough*, 1989]. Owing to the positive correlation between Ce/Pb and U/Pb ratios (Figure 8a), this feature is probably related to, on average, higher Pb abundances in the EM sources relative to the HIMU sources. As noted by *Hofmann* [2004] and *Stracke et al.* [2003b], systematic variations in Ce/Pb (Nd/Pb) ratios in OIB and MORB are therefore resolvable, although the average Ce/Pb ratio of our entire data set is still approximately consistent with the "canonical" value of Ce/Pb = 25 [*Hofmann et al.*, 1986; *Newsom et al.*, 1986]. EM basalts have consistently higher Rb/Sr ratios and lower Lu/Hf but similar Nd/Hf ratios compared to HIMU basalts (Figure 11). Fractionation during partial melting and/or crystallization could be responsible for some of the scatter of the parent/daughter ratios Rb/Sr, Lu/Hf, and also U/Pb. However, the overall positive trends in $^{238}U/^{204}Pb$ versus $^{206}Pb/^{204}Pb$ and $^{87}Rb/^{86}Sr$ versus $^{87}Sr/^{86}Sr$ space (Figure 14) are in good agreement with the isotope systematics, indicating that the EM sources developed with lower time-integrated $^{238}U/^{204}Pb$ and higher time-integrated $^{87}Rb/^{86}Sr$ ratios than the HIMU sources.

[24] Given the overall similar La/Sm ratios in all investigated OIB suites and the general trend of

increasing parent-daughter ratios with increasing corresponding isotope ratio (Figure 14), the systematic differences in Th/U, U/Pb, and Rb/Sr ratios between the EM and the HIMU sources are too large to be explained by partial melting processes alone. The complex enrichment and depletion patterns of the very incompatible elements in EM basalts (especially for Ba and U) are source-dependent (Figure 5), and are contrasted by the regular variation of the bulk partition coefficient values and the mobility factors for the elements between U and Rb (Figure 12). Coupled to the limited compositional variability of the oceanic crust, these observations suggest that more complex processes, possibly involving an additional (variably enriched) source component, must be responsible for the irregular variation of the highly incompatible trace elements and their ratios in EM sources (see discussion above).

[25] On the other hand, the distinct isotope trends of EM-1 and EM-2 basalts indicate that at least two general patterns exist with respect to the long-term evolution of parent/daughter ratios (e.g., Rb/Sr, Sm/Nd, U/Pb, Th/Pb) in the EM sources. Despite these similarities in parent/daughter ratios, other incompatible trace element ratios in the EM sources from one isotopic family (EM-1 or EM-2, respectively) are variable, and compositional differences between *individual* EM-1 and EM-2 are observed, which are ultimately related to different source compositions. Compare, for example, the variation in Rb/La, Ba/La (Figures 10b and 10c), and U/Th ratios (Figure 11f) in samples from the EM-1 islands Gough, Tristan and Pitcairn. The very incompatible trace element systematics therefore suggest that there are many, not only two, EM sources [see also *Sun and McDonough*, 1989], whereas the isotopic relationships could be explained by a minimum of two enriched mantle components (EM-1 and EM-2). Identification of processes leading to sources that evolve, with time, along two distinct isotope paths but retain different incompatible element contents could resolve this apparent conundrum.

[26] The chemical heterogeneity in the Earth's mantle, as witnessed by the chemical and isotopic composition of OIB, must be directly related to interaction between two or several of the Earth's major lithophile element reservoirs (oceanic and continental crust and lithosphere, Earth's mantle). In the discussion above, we have advocated recycling of ancient subduction-modified oceanic lithosphere as the principal mechanism for generating the HIMU reservoir. There is ample evidence for alteration and subduction of oceanic lithosphere, so that this is a geochemically, geologically, and physically plausible scenario. In the following, we will discuss potential scenarios for the origin of EM sources.

5.2.1. Sediment Recycling

[27] On the basis of their isotopic composition, the presence of recycled sediments and oceanic crust in EM sources was invoked more than 20 years ago [*Hawkesworth et al.*, 1979; *Cohen and O'Nions*, 1982; *White and Hofmann*, 1982; *White*, 1985; *Zindler and Hart*, 1986; *Wright and White*, 1987]. Subsequently, *Weaver* [1991] proposed, on the basis of the trace element systematics in OIB, that recycling oceanic crust plus ancient (1–2 Ga) "pelagic" sediments generates EM-1 sources, whereas recycling oceanic crust plus ancient "terrigenous" sediments generates EM-2 sources. This scenario has evolved into somewhat of a paradigm for explaining the geochemical and isotope systematics in OIB [*Hart*, 1988; *Woodhead and McCulloch*, 1989; *Barling and Goldstein*, 1990; *Le Roex et al.*, 1990; *Chauvel et al.*, 1992; *Hauri and Hart*, 1993; *Weis et al.*, 1993; *Woodhead and Devey*, 1993; *Hemond et al.*, 1994; *Roy-Barman and Allègre*, 1995; *Hauri et al.*, 1996; *White and Duncan*, 1996; *Hofmann*, 1997, 2004; *Rehkämper and Hofmann*, 1997; *Blichert-Toft et al.*, 1999; *Eisele et al.*, 2002]. More recently, *Plank and Langmuir* [1998] have shown that the large range in chemical composition in modern marine sediments is mainly governed by the variable proportions of their different lithological constituents (clastic, biogenic, hydrothermal), and is not related in any systematic way to their depositional environment or provenance ("pelagic" and "terrigenous"). Thus different types of marine sediments have overlapping chemical compositions [*Plank and Langmuir*, 1998]. Overall, marine sediments are characterized by a unimodal distribution of their parent-daughter ratios (Figure 15) [see also *Stracke et al.*, 2003a] with average values similar to those of the average upper continental crust [*Taylor and McLennan*, 1985; *Plank and Langmuir*, 1998]. Note that, due to the possible lack of biogenic sediments, Archean or early Proterozoic sediments are likely to be dominated by clastic constituents and are thus expected to be compositionally even closer to the upper continental crust than present-day sediments.

[28] Subducted sediments contain large amounts of water. Dehydration and partial melting during subduction therefore causes large parts of the

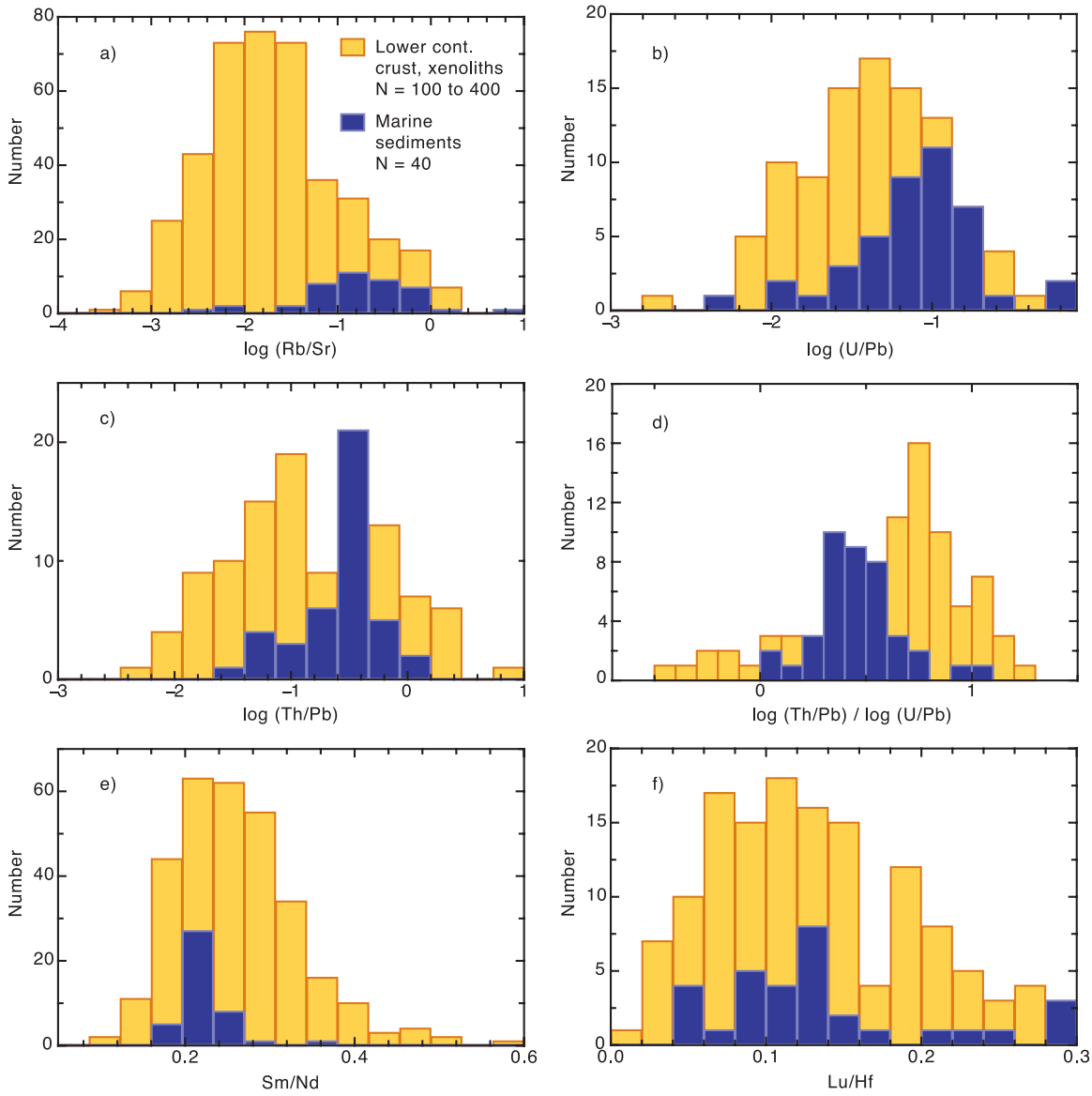

Figure 15. Histograms showing the distribution of parent/daughter ratios of isotope decay systems in presently subducted sediments (data from *Plank and Langmuir* [1998]). Also shown are distributions of the parent/daughter ratios in xenoliths from the lower continental crust (data from compilation of *Rudnick and Gao* [2004]). Due to the large compositional range of the continental crust, some ratios have been plotted in logarithmic scale. Both sets display unimodal patters, though with significantly different maxima for Rb/Sr, U/Pb, Th/Pb, and (Th/Pb)/(U/Pb) ratios, with the exception of Sm/Nd and Lu/Hf ratios.

original sediment signature to be lost, which is obvious from the chemical composition of island arc volcanics, in particular the ^{10}Be abundances and the Th/Rb and Th/La ratios [*White and Dupré*, 1986; *Morris et al.*, 1990; *Stern and Kilian*, 1996; *Elliot et al.*, 1997; *Hoogewerf et al.*, 1997; *Tatsumi*, 2000; *Plank*, 2005] and from recent experimental data [e.g., *Nichols et al.*, 1994; *Stalder et al.*, 1998; *Johnson and Plank*, 1999]. Thus there is ample evidence that sediments are recycled back into the mantle. However, the extent to which the original sediment cover survives subarc processing and makes its way into the deeper mantle remains unresolved. The significance of subducted sediments (in composition and mass) for controlling the final chemical composition of the subducted lithosphere is therefore difficult to assess. Nevertheless, recycling of oceanic lithosphere plus overlying sediments appears to be a plausible mechanism for explaining some of the signatures in *individual* EM sources [*Hawkesworth et al.*, 1979; *Cohen and O'Nions*, 1982; *Chauvel et al.*,

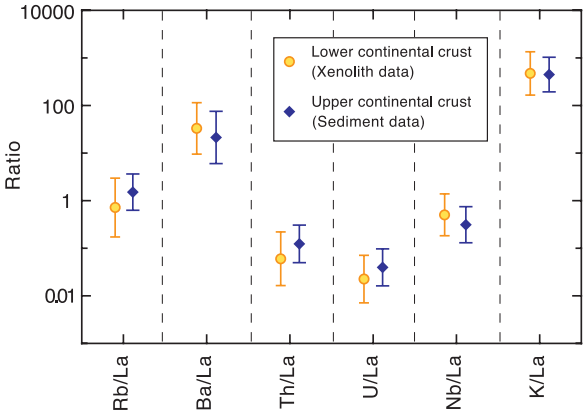

Figure 16. Comparison of very incompatible trace element ratios in the upper and lower continental crust. Averages and variations (1σ) have been calculated using the same data sets as in Figure 15. Note the broad overlap between all these very incompatible trace element ratios in the upper and lower continental crust.

1992; *Weis et al.*, 1993; *Woodhead and Devey*, 1993; *Hemond et al.*, 1994; *White and Duncan*, 1996; *Eisele et al.*, 2002]. Owing to the unimodal distribution of the parent/daughter ratios in marine sediments (Figure 15), however, recycling of sediment cannot account for the two different isotope evolution paths observed in EM sources (EM-1 and EM-2), and so does not provide a suitable explanation for the trace element–isotope conundrum.

5.2.2. Recycling Lower Continental Crust

[29] In $^{87}Sr/^{86}Sr$ - $^{206}Pb/^{204}Pb$ space (Figure 1a), EM-1 and EM-2 sources display distinct, well-defined trends: EM-1 basalts have negative slopes; EM-2 basalts have near vertical or positive slopes. The Rb/Sr ratios in EM-1 sources are therefore negatively coupled to U/Pb ratios, whereas Rb/Sr ratios in EM-2 sources are coupled to relatively constant U/Pb ratios. As a consequence, the time-integrated parent/daughter ratios in EM-1 and EM-2 sources behave in a coherent fashion, despite their variability in other highly incompatible trace element ratios. This behavior is most easily explained in case the processes that lead to this coherent fractionation of the parent/daughter ratios allow for different fractionation and/or preservation of different initial very incompatible trace element ratios.

[30] Intracrustal differentiation has led to the formation of two chemically heterogeneous, but distinct, crustal reservoirs: the lower and the upper continental crust [e.g., *Taylor and McLennan*, 1985; *Rudnick and Fountain*, 1995; *Rudnick and Gao*, 2004]. These differentiation processes, caused by a variety of magmatic and nonmagmatic processes, have led to variable but systematic differences in the trace element abundances of the upper and lower continental crust [*Rudnick and Gao*, 2004]. However, ratios of very incompatible elements or elements with similar geochemical behavior should be less affected than ratios between elements with higher compatibility contrasts or different geochemical behavior (see discussion above). Figure 15 shows the variation in parent/daughter ratios for xenoliths from the lower continental crust (data compilation from *Rudnick and Gao* [2004]) and subducted sediments (data from *Plank and Langmuir* [1998]), which serve as proxies for the average composition of the upper continental crust. There are significant differences in the distribution patterns and maxima for parent/daughter ratios in the upper and lower continental crust resulting in an overall bimodal distribution pattern (Figure 15). These differences cause the upper and lower continental crust to develop, over time, along two different isotope evolution paths. Owing to its lower Rb/Sr and (Th, U)/Pb ratios and higher Th/U ratios, the lower crust develops consistently lower $^{87}Sr/^{86}Sr$, $^{206}Pb/^{204}Pb$, and $^{208}Pb/^{204}Pb$ and higher $^{208}Pb^*/^{206}Pb^*$ ratios than the upper continental crust. This is in good agreement with the systematic isotopic differences between EM-1 and EM-2 basalts (EM-1 have lower $^{87}Sr/^{86}Sr$, $^{206}Pb/^{204}Pb$, and $^{208}Pb/^{204}Pb$ and higher $^{208}Pb^*/^{206}Pb^*$ isotope ratios than EM-2 basalts; Figure 1). Very incompatible trace element ratios in both the upper and lower continental crust, on the other hand, are variable but overlap considerably (Figure 16). Thus, although there are systematic differences in the parent/daughter ratios of the upper and lower continental crust, the two crustal reservoirs are not clearly distinguishable on the basis of their very incompatible trace element ratios.

[31] These characteristics of the upper and lower continental crust may thus provide a possible solution to the trace element–isotope conundrum in EM sources. Mixing small amounts of predominantly lower and upper continental crust (or ancient subducted sediment), respectively, to altered oceanic lithosphere is expected to result in two different isotope evolution paths (EM-1 and EM-2; see also discussion by *Zindler and Hart* [1986]), while preserving similar, but variable very incompatible trace element signatures.

5.2.3. Mixing Relationships

[32] The trace element composition of EM-1 and EM-2 basalts, especially the relative enrichment in

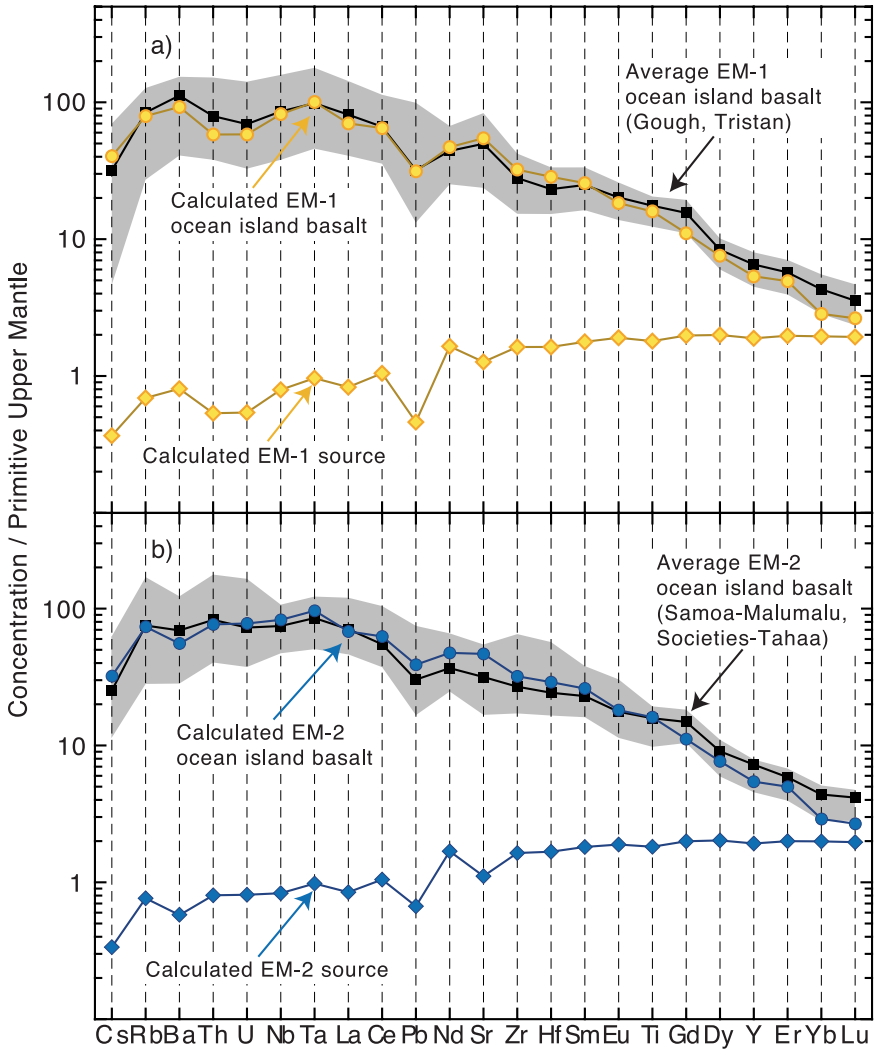

Figure 17. (a) Calculated trace element patterns of average EM-1 basalt assuming melting of a subducted package consisting of 90% depleted lithospheric mantle [*Salters and Stracke*, 2004], 9% oceanic crust [*Sun and McDonough*, 1989; *Staudigel et al.*, 1996; *Hart et al.*, 1999], and 1% lower continental crust [*Rudnick and Gao*, 2004], followed by nonmodal accumulated fractional melting of garnet-peridotite source (F = 0.01). (b) Calculated trace element patterns of average EM-2 basalt assuming melting of a subducted package consisting of 90% depleted lithospheric mantle, 9.8% oceanic crust, and 0.2% upper continental crust [*Taylor and McLennan*, 1985], followed by nonmodal accumulated fractional melting of garnet-peridotite source (F = 0.01). The degree of melting is largely dependent on the assumed trace element content of the oceanic lithospheric mantle. Higher concentrations permit higher degrees of melting (compare to Figures 9 and 14). Also shown are the averages and ranges of (a) Gough and Tristan basalts and (b) Samoa-Malumalu and Societies-Tahaa basalt. See Appendix B for a more detailed description of the model.

very incompatible trace elements, the less pronounced Nb-Ta enrichment and Pb depletion compared to HIMU basalts, is modeled quantitatively by mixing subducted oceanic lithosphere with lower and upper continental crust, respectively (Figure 17). Calculations are done on the basis of the model described in detail by *Stracke et al.* [2003a]. More detailed descriptions of the calculations are given in Appendix B and the caption of Figure 17. Modeling of the isotopic composition of EM-1 and EM-2 basalts, using the same compositions and mixing proportions as for the trace elements also successfully reproduces the isotopic compositions of EM-1 and EM-2 basalts [*Stracke et al.*, 2004]. This is in good agreement with the conclusions of *Escrig et al.* [2004] and *Hanan et al.* [2004], who suggested that the EM-like isotope signatures in Indian MORB are consistent with the presence of delaminated lower continental crust in the sub-Indian Ocean mantle.

[33] In Ba/Rb versus Th/Rb space (Figure 18), all OIB form a roughly triangular pattern with the EM

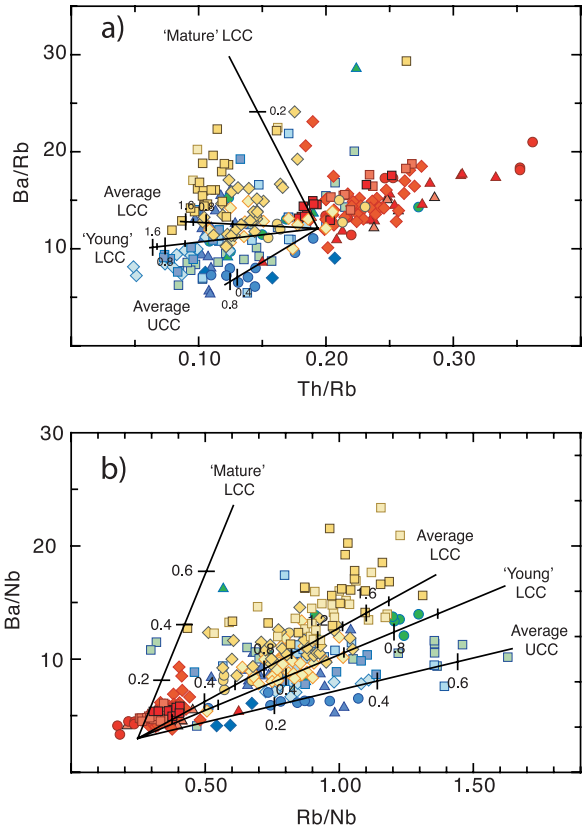

Figure 18. Data for basalts in (a) Ba/Rb versus Th/Rb and (b) Ba/Nb versus Rb/Nb space. Modeled mixing trajectories have been calculated assuming the same model as in Figure 17. The large variation in trace element ratios within single suites can be explained by mixing up to 2% of lower continental crust (LCC) with different bulk composition (average, young, and mature lower continental crust) and up to 1% average upper continental crust (UCC). See Appendix B for a more detailed description of the model. Note that, with a few exceptions, the trends of individual suites run oblique to the trajectories of HIMU-lower/upper continental crust, suggesting that each suite contains a rather fixed mixture of recycled oceanic lithosphere (HIMU) and heterogeneous continental material. Symbols same as in Figure 6.

basalts (large spread in Ba/Rb at low Th/Rb) fanning out from the HIMU basalts at the apex with high values for Th/Rb and intermediate values for Ba/Rb. Interestingly, the individual arrays of most EM-type suites do not trend toward the HIMU field, but are, with some exceptions, more or less oblique to it (see for example the suites of Gough and Tristan basalts in Figure 18a). Similar patterns are observed for other trace element ratios (e.g., Ba/Nb versus Rb/Nb; Figure 18b) or isotopes (e.g., $^{208}Pb/^{204}Pb$ versus $^{206}Pb/^{204}Pb$ isotopes, not shown). These patterns are consistent with mixing recycled oceanic lithosphere with relatively *constant* proportions of compositionally *heterogeneous* upper or lower continental crust. Thus each EM source reflects its own unique composition, determined by (1) rather *constant* proportions of recycled oceanic lithosphere and continental crust and by (2) *variable* mixtures of composotionally different lithologies of continental crust. In contrast to the HIMU signature (see discussion in section 5.1), therefore, the EM signature does not appear to be related to a small number of concrete reservoirs (i.e., two) in the mantle, but appears to be related to different sources that are produced in the same general manner, but with different proportions of a limited number of heterogeneous constituents.

5.2.4. Mechanisms for Recycling Lower Continental Crust

[34] The preceding discussion shows that the trace element and isotope systematics of EM-1 and EM-2 basalts can be explained by recycling oceanic lithosphere and various proportions of lower and upper continental crust, respectively, but leaves one important question unanswered: How can the lower continental crust, together with subduction-modified oceanic lithosphere, be recycled into the mantle?

[35] Delamination of the lower continental crust has previously been proposed [*Tatsumoto and Nakamura*, 1991; *Kay and Kay*, 1993; *Rudnick*, 1995; *Tatsumi and Kogiso*, 1997; *Escrig et al.*, 2004; *Hanan et al.*, 2004]. Although this is certainly a viable process, delamination of the lower continental crust without the attached subcontinental lithospheric mantle [*Escrig et al.*, 2004] may require special conditions [*Jull and Kelemen*, 2001]. Although the composition of the subcontinental lithospheric mantle is hard to constrain, it appears to have a characteristically unradiogenic $^{187}Os/^{188}Os$ signature [*Pearson et al.*, 2004]. The lack of such unradiogenic $^{187}Os/^{188}Os$ signatures in OIB suggests that the subcontinental lithospheric mantle is not a major constituent of present OIB sources [e.g., *Eisele et al.*, 2002; *Escrig et al.*, 2004]. The apparent presence of subduction-modified oceanic lithosphere in the EM sources (see preceding discussion) also implies that subduction zone mechanisms rather than delamination must be responsible for introducing the lower continental crust into the mantle.

[36] Recent bathymetric and structural studies stress the importance of erosive versus accretionary convergent margins for the global mass flux at subduction zones (for recent reviews, see *Clift and*

Vannucchi [2004], *von Huene et al.* [2004], and *Vannucchi et al.* [2004]). Prolonged bending of the oceanic crust during subduction causes rocks at the base of the upper plate to be fractured and dragged into the subduction channel where they are subducted together with the oceanic crust and attached lithospheric mantle [*von Huene et al.*, 2004]. Mass flux calculations suggest erosion rates of the overriding continental crust of up to 100 km^3 per million years [*Clift and Vannucchi*, 2004]. Erosive margins are characterized by net-loss of continental crust to the mantle, high orthogonal convergence rates and a thin sediment veneer on the subducted oceanic plate. The latter is probably related to the short transient time of the oceanic plate through the forearc region. Accretionary margins are characterized by net-growth of continental crust, slow convergence rates and long transient times of the oceanic plate through the forearc, which cause accumulation of thick piles of continentally derived sediments in accretionary prisms. Thus the loss of continental crust by subduction is balanced by crustal accretion through sediment underplating and arc volcanism. Nevertheless, crustal material is recycled at both erosive and accretionary margins.

[37] Recycling of continental crust through subduction erosion not only provides a valid mechanism for recycling of continental material, it is also consistent with the inferred additional presence of subduction-modified oceanic lithosphere in EM sources (see discussion above), and is therefore chemically, geologically, and physically plausible. More speculatively, recycling of continental crust via subduction erosion might also be a possible explanation for the bimodal pattern of EM signatures in isotope space (EM-1 and EM-2). EM-1 sources could be created predominantly at erosive margins through preferential erosion and recycling of lower crustal material, whereas a EM-2 sources could be formed predominantly at accretionary margins through preferential recycling of continentally derived sediments and/or eroded upper continental crust. Whether sediment subduction or erosion of upper crust is more important is hard to assess.

5.3. Alternative Scenarios: Metasomatic Processes

[38] *Tatsumi* [2000] suggested that EM-1 sources are formed by pyroxenitic restites that delaminate during the anatexis of lower continental crust at destructive plate margins. The modeled trace element composition of the pyroxenitic source of *Tatsumi* [2000] is, however, highly enriched in very incompatible elements relative to LREE, has a pronounced negative Nb anomaly (relative to La) and a large positive Pb anomaly relative to Ce [see *Tatsumi*, 2000, Figure 2]. These features are inconsistent with the flat but irregularly shaped very incompatible trace element pattern, the positive Nb anomaly and the negative Pb anomaly of all OIB investigated in this study.

[39] Recently, metasomatic processes involving low-degree partial melts have been suggested as possible mechanisms to explain the enriched trace element and isotope signatures of OIB in general [*Niu and O'Hara*, 2003] and the EM-2 signatures of Samoan basalts in particular [*Workman et al.*, 2004]. The systematic isotopic diversity of OIB mantle components (HIMU, EM-1 and EM-2), however, would require a range of different but systematic and reproducible metasomatic processes that is difficult to imagine on the basis of our, albeit limited, knowledge of potential suboceanic metasomatic processes (see discussion below). For the specific case of Samoa, the EM-2 isotope signature of the Samoan lavas is successfully explained by the metasomatic model presented by *Workman et al.* [2004]. The smoothly increasing incompatible trace element concentrations from La to Cs in the proposed Samoan EM-2 source [see *Workman et al.*, 2004, Figure 20], however, are irreconcilable with the irregular and shallowly sloped incompatible trace element pattern of the Samoan basalts (low (Cs, Ba, U, K)/La and high (Th, Rb)/La ratios). If anything, melting of the proposed EM-2 source would lead to an even steeper sloped incompatible trace element pattern. Thus additional components and/or processes must be involved in the generation of the Samoan lavas.

[40] Fluid-rock or low-degree melt-rock interaction in the oceanic lithosphere is perhaps a widespread phenomenon and may contribute to the compositional variability of some OIB sources. However, our understanding of the chemical composition of potential metasomatic agents and metasomatized materials, the scale of such processes and the ways by which metasomatized material may end up as source material for OIB remains limited and is characterized by uncertainties probably similar to or even exceeding those related to recycling of oceanic lithosphere plus continental crust. Geochemically, it is difficult to assess whether recycling of oceanic lithosphere plus continental crust or interaction of essentially basaltic melts with the depleted oceanic lithosphere is responsible for the enriched signatures in some of the OIB sources. While there is ample evidence of subduction of oceanic lithosphere and continental material (at

least to upper mantle levels) from both observations and mass balance calculations [*Clift and Vannucchi*, 2004], evidence for widespread fluid/melt-rock interactions in the suboceanic mantle is ambiguous. We therefore favor recycling of oceanic lithosphere with or without continental material as the principal mechanism for introducing chemical heterogeneity into the Earth's mantle.

6. Conclusions

[41] The systematic analysis of ocean island basalts representing the most extreme isotopic mantle end-members (HIMU, EM-1 and EM-2) corroborates existing models that recycled oceanic lithosphere provides a pivotal role in the evolution of their sources, but also requires the presence of at least two additional and heterogeneous crustal components: the upper and lower continental crust.

[42] The uniform trace element composition of all HIMU basalts in combination with their comparatively small range in isotopic composition suggest that the HIMU sources must have evolved with remarkably uniform and depleted composition for similar time periods, *irrespective* of their inferred origin. The characteristic relative enrichments and depletions of incompatible trace elements in HIMU basalts and their sources in combination with their unique isotope signatures are shown to be quantitatively compatible with recycling of subduction-modified oceanic lithosphere without significant contribution from other components.

[43] Similar trace element ratios in EM and HIMU basalts (La/Th, Sr/Nd, (Rb, Ba)/K) suggest that subduction-modified oceanic lithosphere is also likely to be involved in the genesis of EM sources. At the same time, the systematically higher Th/U and Rb/Sr ratios and the less pronounced Pb depletion, which translate into the more radiogenic Sr but less radiogenic Pb isotope signatures, and the generally more enriched and more variable incompatible trace element abundances (Cs, Rb, Ba, Th, U, Nb, Ta, K, La) of EM relative to HIMU basalts require additional heterogeneous components in their sources.

[44] Subducted oceanic sediment can explain some of the chemical variability of EM(-2) basalts but cannot be responsible for the binary isotopic trends of EM-1 and EM-2 basalts because the compositional distribution of subducted sediment, at least with respect to parent-daughter ratios, is unimodal and on average similar to that of the upper continental crust. In contrast, the differences in parent/daughter ratios between the upper and lower continental crust in combination with high recycling ages (on the order of 10^9 years), and the similar but variable incompatible trace element ratios of the upper and lower continental crust, match both the isotopic and trace element characteristics observed in EM-type basalts. Therefore recycling of upper and lower continental crust via subduction erosion at erosive plate margins (and possibly by sediment subduction) in various proportions to the oceanic lithosphere can produce the diverging isotopic trends in EM-1 and EM-2 basalts while maintaining the observed large, but similar variance in the trace element composition of EM basalts. In contrast to the HIMU source, the EM signature consequently does not appear to be related to two concrete reservoirs (EM-1 and EM-2) in the mantle, but seems to be related to different sources that are produced in the same general manner, but with by different proportions of a limited number of heterogeneous constituents.

Appendix A: Analytical Techniques

[45] New high-precision major and trace element data on OIB from the islands of St. Helena, Gough and Tristan in the Atlantic Ocean are presented in Table 1. Sample powders were prepared in an agate shatter box. Major elements have been determined by XRF at the University of Mainz. The concentrations of Sr, Zr, Ba, Nd, Sm, Hf, Pb, and U have been measured by isotope dilution (ID)-ICPMS at the MPI [*Willbold and Jochum*, 2005]. The remaining trace element concentrations were determined by laser ablation (LA)-ICPMS using a ThermoFinnigan ELEMENT 2 mass spectrometer coupled to a New Wave UP-213 laser ablation system. LA-ICPMS measurements were done on glass beads made from about 50 mg of sample powder using an electronically controlled iridium strip heater (K. P. Jochum et al., Trace element and isotope analyses of geo- and cosmological samples by laser ablation-sector field-ICPMS, submitted to *High Resolution ICPMS*, 2004). The NIST SRM 612 has been used for calibration [*Pearce et al.*, 1997]. The MPI-DING reference glasses KL2-G and ML3B-G [*Jochum et al.*, 2000] and the USGS reference material BHVO-1 have been used for quality assurance (Table A1). Conventionally, Ca is used as an internal standard element for LA-ICPMS measurements. By using the eight trace elements previously determined by ID-ICPMS (Sr, Zr, Ba, Nd, Sm, Hf, Pb, and U), an up to three-fold improvement in both accuracy and reproducibility can be achieved compared to using Ca only. The

Table A1. Trace Element Concentrations in Reference Materials Determined by ID-LA-ICPMS[a]

	Sample					
	BHVO-1 (n = 12)		KL2-G (n = 7)		ML3B-G (n = 7)	
	Average	1 σ	Average	1 σ	Average	1 σ
Rb	9.42	0.33	8.54	0.27	5.85	0.06
Sr	401	8	372	7	318	6
Y	27.1	0.4	27.9	0.3	26.8	0.0
Zr	173	3	160	3	131	1
Nb	17.6	0.5	14.7	0.8	8.18	0.10
Cs	0.096	0.004	0.122	0.005	0.141	0.005
Ba	135	2	125	2	81.5	1.0
La	15.8	0.1	13.6	0.2	9.54	0.04
Ce	37.5	0.4	32.3	0.3	23.3	0.2
Pr	5.33	0.03	4.65	0.04	3.45	0.01
Nd	24.9	0.2	22.1	0.20	17.2	0.3
Sm	6.08	0.12	5.63	0.11	4.79	0.05
Eu	2.09	0.02	1.97	0.03	1.72	0.01
Gd	6.32	0.09	6.09	0.19	5.59	0.03
Tb	0.915	0.014	0.905	0.024	0.847	0.012
Dy	5.54	0.10	5.57	0.20	5.35	0.07
Ho	1.01	0.02	1.03	0.04	1.01	0.01
Er	2.60	0.06	2.67	0.11	2.66	0.02
Tm	0.323	0.005	0.344	0.007	0.326	0.002
Yb	2.02	0.02	2.15	0.06	2.07	0.03
Lu	0.265	0.003	0.283	0.001	0.277	0.002
Hf	4.24	0.08	3.98	0.08	3.23	0.06
Ta	1.14	0.02	0.962	0.048	0.530	0.003
W	0.204	0.044	0.406	0.015	0.303	0.016
Pb	2.10	0.04	2.08	0.04	1.40	0.03
Th	1.21	0.04	0.924	0.023	0.576	0.021
U	0.409	0.004	0.538	0.005	0.430	0.004

[a] Concentrations are in μg/g.

reproducibility (as determined by 12 independent measurements of BHVO-1) is better than 2% (RSD) for all elements except for Rb and Th (both 3% RSD) and Cs (4% RSD). The accuracy, determined relative to literature data for BHVO-1 [*Govindaraju*, 1994; *Jochum et al.*, 2001; *Raczek et al.*, 2001], is better than 2% with the exception of Cs, Tb, and Ho (about 5%). The combined standard uncertainty of the determined concentrations, which, among others, includes uncertainty of measurement, sample heterogeneity, uncertainty of spike concentrations, and uncertainty of calibration factors, is less than 2% (RSD) for elements determined by ID (Sr, Zr, Ba, Nd, Sm, Hf, Pb, and U) and less than 5% (RSD) for all remaining lithophile elements [*Willbold et al.*, 2003].

Appendix B: Quantitative Modeling

B1. Model Parameters

[46] The calculations and parameters used in the modeling of OIB sources (Figure 17; partition coefficients, fluid-mobility factors, mineral and melting modes) are published in *Stracke et al.* [2003a]. Assuming different sets of partition coefficients, mineral and melting modes (see references given in Figure 9) does not significantly change the results of the calculations as demonstrated in Figures 9 and 12. For the generation of the trace element characteristics of the EM sources (Figure 17), it is assumed that depleted lithospheric mantle [*Salters and Stracke*, 2004] together with oceanic crust consisting of a mixture of 40% MORB [*Sun and McDonough*, 1989], 50% gabbro [*Hart et al.*, 1999], 10% altered MORB [*Staudigel et al.*, 1996] and with fragments of eroded lower continental crust and sediments (upper continental crust) are recycled into the mantle (see section B2 for input compositions). Subducted sediments are water-barren and we therefore assume that the sediment component is modified by partial melting during subduction [e.g., *Hoogewerf et al.*, 1997; *Nichols et al.*, 1994]. Owing to tectonic stress induced at subduction zones, the lower continental crust is likely to be fractured [*von Huene et al.*, 2004], thus promoting the canalization of the fluid and reducing the quantitative interaction between

Table B1. Trace Element Concentrations of Components Used for Modeling[a]

	Depleted Mantle	N-MORB	Altered MORB	Gabbro	Average Upper Continental Crust		Average Lower Continental Crust		Mature Lower Continental Crust		Young Lower Continental Crust		Lower Continental Crust Estimates		
													Rudnick and Gao [2004]		
	Salters and Stracke [2004]	*Sun and McDonough* [1989]	*Staudigel et al.* [1996]	*Hart et al.* [1999]	Used in Model	*Taylor and McLennan* [1985]	Used in Model	*Rudnick and Gao* [2004]	Used in Model	*Weaver and Tarney* [1984]	Used in Model	*Villaseca et al.* [1999]	Min.	Med.	Max.
Ti	798	7600	7074	8045	3837	3837	4916	4916	2997	2997	6234	6234	2997	5396	7973
Rb	0.09	0.56	9.6	0.56	112	112	17	11	14	11	50	90	7.0	25	90
Sr	9.8	90	115	158	450	350	348	348	400	569	286	286	196	350	712
Zr	7.9	74	67	78	190	190	86	86	202	202	206	206	68	121	206
Y	4.1	28	27	27	22	22	16	16	7.0	7.0	40	40	7	18	40
Nb	0.21	2.3	1.2	1.7	12	12	5.0	5.0	5.0	5.0	15	15	5.0	6.6	15
Cs	0.001	0.007	0.15	0.019	1.0	4.6	0.30	0.30	0.07	0.07	0.07	0.07	0.07	0.30	2.6
Ba	1.20	6.3	22.6	9.5	550	550	259	259	757	757	500	994	150	516	1434
La	0.23	2.5	1.8	4.8	30	30	8.0	8.0	22	22	38	38	8.0	20	38
Ce	0.77	7.5	6.0	15	64	64	20	20	44	44	73	73	20	40	73
Nd	0.71	7.3	6.6	10	35	26	12	11	19	19	30	30	2.8	18	30
Sm	0.27	2.6	2.5	3.1	4.3	4.5	2.0	2.8	3.3	3.3	6.0	6.6	1.1	3.7	6.6
Eu	0.11	1.0	0.91	1.1	0.88	0.88	1.1	1.1	1.2	1.2	1.8	1.8	1.0	1.3	3.6
Gd	0.40	3.7	3.7	4.1	3.8	3.8	3.1	3.1	3.1	3.1	6.8	6.8	0.48	3.7	6.8
Dy	0.53	4.6	4.4	5.0	3.5	3.5	3.1	3.1	2.5	2.5	6.7	6.7	0.60	3.6	6.7
Er	0.37	3.0	2.8	2.8	2.3	2.3	1.9	1.9	1.3	1.3	4.2	4.2	1.3	2.2	4.2
Yb	0.40	3.1	2.7	2.8	2.2	2.2	1.5	1.5	1.2	1.2	4.0	4.0	0.79	1.9	4.0
Lu	0.063	0.46	0.43	0.40	0.32	0.32	0.25	0.25	0.18	0.18	0.65	0.65	0.12	0.29	0.65
Hf	0.20	2.1	1.9	2.1	5.8	5.8	1.9	1.9	3.6	3.6	6.0	6.0	1.9	2.8	6.0
Ta	0.014	0.13	0.10	0.11	2.0	2.0	0.60	0.60	0.70	0.70	0.70	0.70	0.21	0.60	1.3
Pb	0.023	0.30	0.24	0.60	18.0	17.0	3.0	4.0	5.0	13.0	5.0	(-)	3.0	5.0	13.0
Th	0.014	0.12	0.07	0.16	10.7	10.7	1.3	1.2	0.42	0.42	2.7	5.7	0.42	1.4	6.6
U	0.005	0.047	0.30	0.044	2.5	2.8	0.27	0.20	0.05	0.05	0.47	0.47	0.05	0.34	1.4

fluid released from the subducted slab [*Breeding et al.*, 2003; *Ague*, 2004]. Therefore the bulk chemical composition of the eroded lower crust is likely to be unaffected by subduction zone alteration processes.

[47] A recycling age of 2 Ga, and partial melting (F = 0.01) of a subducted package consisting of 90% depleted lithospheric mantle [*Salters and Stracke*, 2004] and 9% oceanic crust [*Sun and McDonough*, 1989; *Staudigel et al.*, 1996; *Hart et al.*, 1999] and 1% lower continental crust [*Rudnick and Gao*, 2004] for EM-1 and 9.8% oceanic crust and 0.2% upper continental crust [*Taylor and McLennan*, 1985] for EM-2, respectively, is assumed for the calculations in Figure 17 (see Table B1 for all input compositions). The assumed degree of partial melting of this overall garnet-peridotitic source depends largely on the concentrations of the depleted oceanic lithosphere. Higher concentrations in the oceanic lithosphere permit higher degrees of partial melting (compare to Figures 9a and 12a).

B2. Composition of the Recycled Continental Components

[48] The average chemical composition of the upper continental crust is taken from *Taylor and McLennan* [1985]. Different analytical approaches (geochemical data, seismic data, heat flow data, etc.) on different materials (sediments, granulites, xenoliths, etc.) from various regions of the Earth have been used to estimate the average compositions of the lower continental crust [see *Rudnick and Gao*, 2004]. The different average compositions are taken to represent viable approximations for the large-scale compositional variation within the lower continental crust. The average overall chemical composition of the lower continental crust used for the calculations in Figure 17 is taken from *Rudnick and Gao* [2004]. The lower crustal composition by *Weaver and Tarney* [1984] is used as an estimate for an evolved composition of the lower continental crust. This estimate is based on granulite data from the Lewisian complex, Scotland. It has a composition similar to tonalite-trondhjemite-granodiorite assemblages [*Rudnick and Gao*, 2004] and may therefore be representative for stabilized, mature continents. The lower crustal composition by *Villaseca et al.* [1999] is used as an estimate for an extremely felsic composition of the lower continental crust. It has high SiO_2 and K_2O content similar to that of the upper continental crust and is considered to be representative for young lower crust [*Rudnick and Gao*, 2004].

[49] Some of the trace element compositions of the average crust compositions are slightly modified to account for the isotope and element compositions of the EM basalts (Table B1). Most modifications were done for the parent/daughter elements of the isotope decay systems (U, Th, Pb, Lu, Hf, Rb, Sr, Sm, Nd), but were kept as small as possible (Table B1) and are usually within the given uncertainty. It should be noted that the present-day isotopic composition is not only a function of the abundance of parent and daughter elements, but also of time. Thus all modifications done for the parent/daughter concentrations are arbitrary since the exact age of the recycled components is unknown (a recycling age of 2 Ga is assumed in all calculations). Nevertheless, the absolute concentrations of the modified parent/daughter elements lie well within the given range of all estimates. To illustrate this, the median, maximum and minimum values of estimated element concentration in the lower crust using the data compilation given by *Rudnick and Gao* [2004] are given in Table B1.

[50] In detail, U, Nd, Sr, Sm concentrations are modified by less than 20% in the upper continental crust [*Taylor and McLennan*, 1985], Cs has been reduced from 4.6 to 1 μg/g to be compatible with the low Cs concentration in EM-2 basalts. The changes of the parent/daughter element concentrations in the average lower continental crust [*Rudnick and Gao*, 2004] range between 5 and 40% (Pb 50%; Table B1). In the mature lower crust [*Weaver and Tarney*, 1984], Rb has been increased by 20% and Sr reduced by 40%. Lead has been reduced from 13 to 5 μg/g. Note that the Pb value given by *Weaver and Tarney* [1984] seems unrealistically high, especially if these parts of the lower crust have experienced long-term magmatic and hydrothermal modification. Assuming a Pb value of 5 μg/g results in a Ce/Pb ratio of 8.8, which is in better accordance with the Pb value of 7.5 by *Shaw et al.* [1994] that has also been derived from granulites. The Rb, Ba, and Th concentrations in the young lower crust [*Villaseca et al.*, 1999] are the highest of all lower crustal estimates given by *Rudnick and Gao* [2004] and have been lowered considerably (Rb from 90 to 50 μg/g, Ba from 994 to 500 μg/g, and Th from 5.8 to 2.7 μg/g). Nevertheless, the modified concentrations are still higher than all other estimates and may thus be representative of an extreme end-member of the lower crustal composition. The Sm concentration

has been reduced by 10%, and since *Villaseca et al.* [1999] do not give a Pb concentration, we assumed a U/Pb ratio of 0.1 (that is similar to most other estimates) to estimate the Pb concentration.

Acknowledgments

[51] Marjorie Wilson is thanked for kindly providing the St. Helena samples. Dan McKenzie, Mike Carpenter, and Steve Laurie are thanked for locating and selecting the Gough samples from the Harker Collection at Cambridge University, which were originally collected during the Gough Island Scientific Survey by R. W. LeMaitre in 1956. Dan especially is thanked for doing a great job in selecting the freshest samples available. The Natural History Museum, London kindly donated the Tristan samples, which were originally collected during the Royal Society Expedition to Tristan da Cunha in 1962. Dave Smith from the Natural History Museum, London did an excellent job in selecting a broad spectrum of astonishingly fresh samples. Bill White and Roberta Rudnick are thanked for editorial handling and comments on the manuscript. The authors also thank Al Hofmann for his informal review and the journal reviewers Ken Sims and Yaoling Niu for critical and constructive comments. This work is partly supported by the Deutsche Forschungsgemeinschaft (DFG grant STR853/1 to A.S).

References

Ague, J. J. (2004), Fluid flow in the deep crust, in *Treatise on Geochemistry*, vol. 3, *The Crust*, edited by R. L. Rudnick, pp. 195–228, Elsevier, New York.

Ahrens, L. H. (1954), The lognormal distribution of the elements (A fundamental law of geochemistry and its subsidiary), *Geochim. Cosmochim. Acta*, *5*, 49–73.

Allègre, C. J., B. Dupré, and E. Lewin (1986), Thorium/uranium ratio of the Earth, *Chem. Geol.*, *56*, 219–227.

Anders, E., and N. Grevesse (1989), Abundances of the elements: Meteoritic and solar, *Geochim. Cosmochim. Acta*, *53*, 197–214.

Ayers, J. (1998), Trace element modeling of aqueous fluid-peridotite interaction in the mantle wedge of subduction zones, *Contrib. Mineral. Petrol.*, *132*, 390–404.

Barling, J., and S. L. Goldstein (1990), Extreme isotopic variations in Heard island lavas and the nature of mantle reservoirs, *Nature*, *348*, 59–62.

Blichert-Toft, J., F. A. Frey, and F. Albarède (1999), Hf isotope evidence for pelagic sediments in the source of Hawaiian basalts, *Science*, *285*, 879–882.

Breeding, C. M., J. J. Ague, M. Bröcker, and E. W. Bolton (2003), Blueschist preservation in a retrograded, high-pressure, low-temperature metamorphic terrane, Tinos, Greece: Implications for fluid flow paths in subduction zones, *Geochem. Geophys. Geosyst.*, *4*(1), 9002, doi:10.1029/2002GC000380.

Brenan, J. M., H. F. Shaw, D. L. Phinney, and F. J. Ryerson (1994), Rutile-aqueous fluid partitioning of Nb, Ta, Hf, Zr, U and Th: Implications for high-field strength element depletions in island-arc basalts, *Earth Planet. Sci. Lett.*, *128*, 327–339.

Brenan, J. M., H. F. Shaw, F. J. Ryerson, and D. L. Phinney (1995), Mineral-aqueous fluid partitioning of trace elements at 900°C and 2.0 GPa: Constraints on the trace element chemistry of mantle and deep crustal fluids, *Geochim. Cosmochim. Acta*, *59*, 3331–3350.

Chauvel, C., A. W. Hofmann, and P. Vidal (1992), HIMU-EM: The French Polynesian connection, *Earth Planet. Sci. Lett.*, *110*, 99–119.

Chauvel, C., W. McDonough, G. Guille, R. Maury, and R. Duncan (1997), Contrasting old and young volcanism in Rurutu Island, Austral chain, *Chem. Geol.*, *139*, 125–143.

Clift, P., and P. Vannucchi (2004), Controls on tectonic accretion versus erosion in subduction zones: Implications for the origin and recycling of the continental crust, *Rev. Geophys.*, *42*, RG2001, doi:10.1029/2003RG000127.

Cohen, R. S., and R. K. O'Nions (1982), Identification of recycled continental material in the mantle from Sr, Nd, and Pb isotope investigations, *Earth Planet. Sci. Lett.*, *61*, 73–84.

Eisele, J., M. Sharma, S. J. G. Galer, J. Blichert-Toft, C. W. Devey, and A. W. Hofmann (2002), The role of sediment recycling in EM-1 inferred from Os, Pb, Hf, Nd, Sr isotope and trace element systematics of the Pitcairn hotspot, *Earth Planet. Sci. Lett.*, *196*, 197–212.

Elliot, T., T. Plank, A. Zindler, W. White, and B. Bourdon (1997), Element transport from slab to volcanic front at the Mariana arc, *J. Geophys. Res.*, *102*, 14,991–15,019.

Escrig, S., F. Campas, B. Dupré, and C. J. Allègre (2004), Osmium isotopic constraints on the nature of the DUPAL anomaly from Indian mid-ocean-ridge basalts, *Nature*, *431*, 59–63.

Foley, S. F., M. G. Barth, and G. A. Jenner (2000), Rutile/melt partition coefficients for trace elements and an assessment of the influence of rutile on the trace element characteristics of subduction zone magmas, *Geochim. Cosmochim. Acta*, *64*, 933–938.

Govindaraju, K. (1994), 1994 compilation of working values and sample description for 383 geostandards, *Geostand. Newsl.*, *18*, 1–158.

Halliday, A. N., A. P. Dickin, A. E. Fallick, and J. G. Fitton (1988), Mantle dynamics: A Nd, Sr, Pb, and O isotopic study of the Cammeroon Line Volcanic Chain, *J. Petrol.*, *29*, 181–211.

Hanan, B. B., J. Blichert-Toft, D. G. Pyle, and D. M. Christie (2004), Contrasting origins of the upper mantle revealed by hafnium and lead isotopes from the Southeast Indian Ridge, *Nature*, *432*, 91–94.

Hart, S. (1988), Heterogeneous mantle domains: Signatures, genesis and mixing chronologies, *Earth Planet. Sci. Lett.*, *90*, 273–296.

Hart, S. R., J. Blusztajn, H. J. Dick, P. S. Meyer, and K. Muehlenbachs (1999), The fingerprint of seawater circulation in a 500-m section of ocean crust gabbros, *Geochim. Cosmochim. Acta*, *63*, 4059–4080.

Hart, S. R., and H. Staudigel (1989), Isotopic characterization and significance of recycled components, in *Crust/Mantle Recycling at Convergence Zones*, edited by S. R. Hart and L. Gulen, pp. 15–28, Springer, New York.

Hauri, E. H., and S. R. Hart (1993), Re-Os isotope systematics of HIMU and EMII oceanic island basalts from the south Pacific Ocean, *Earth Planet. Sci. Lett.*, *114*, 353–371.

Hauri, E. H., J. C. Lassiter, and D. J. DePaolo (1996), Osmium isotope systematics of drilled lavas from Mauna Loa, Hawaii, *J. Geophys. Res.*, *101*, 11,793–11,806.

Hawkesworth, C. J., M. J. Norry, J. C. Roddick, and R. Vollmer (1979), $^{143}Nd/^{144}Nd$ and $^{87}Sr/^{86}Sr$ ratios from the Azores and their significance in LIL-element enriched mantle, *Nature*, *280*, 28–31.

Hemond, C., C. W. Devey, and C. Chauvel (1994), Source compositions and melting processes in the Society and Austral plumes (South Pacific Ocean): Element and isotope (Sr, Nd, Pb, Th) geochemistry, *Chem. Geol.*, *115*, 7–45.

Hofmann, A. W. (1997), Mantle geochemistry: The message from oceanic volcanism, *Nature*, *385*, 219–229.

Hofmann, A. W. (2004), Sampling mantle heterogeneity through oceanic basalts: Isotopes and trace elements, in *Treatise on Geochemistry*, vol. 2, *The Mantle and Core*, edited by R. W. Carlson, pp. 61–101, Elsevier, New York.

Hofmann, A. W., and W. M. White (1982), Mantle plumes from ancient oceanic crust, *Earth Planet. Sci. Lett.*, *57*, 421–436.

Hofmann, A. W., K. P. Jochum, H. M. Seufert, and W. M. White (1986), Nb and Pb in oceanic basalts: New constraints on mantle evolution, *Earth Planet. Sci. Lett.*, *79*, 33–45.

Hoogewerf, J. A., M. J. van Bergen, P. Z. Vroon, J. Hertogen, R. Wordel, A. Sneyers, A. Nasution, J. C. Varekamp, H. L. E. Moens, and D. Mouchel (1997), U-series, Sr-Nd-Pb isotope and trace-element systematics across an active island arc-continent collision zone: Implications for element transfer at the slab-wedge interface, *Geochim. Cosmochim. Acta*, *61*, 1057–1072.

Irvine, T. N., and W. R. A. Baragar (1971), A guide to the chemical classification of the common volcanic rocks, *Can. J. Earth Sci.*, *8*, 523–548.

Jochum, K. P., et al. (2000), The preparation and preliminary characterisation of eight geological MPI-DING reference glasses for in-site microanalysis, *Geostand. Newsl.*, *24*, 87–133.

Jochum, K. P., B. Stoll, J. A. Pfänder, M. Seufert, M. Flanz, P. Maissenbacher, M. Hofmann, and A. W. Hofmann (2001), Progress in multi-ion counting spark-source mass spectrometry (MIC-SSMS) for the analysis of geological samples, *Fresenius J. Anal. Chem.*, *370*, 647–653.

Johnson, M. C., and T. Plank (1999), Dehydration and melting experiments constrain the fate of subducted sediments, *Geochem. Geophys. Geosyst.*, *1*(1), doi:10.1029/1999GC000014.

Jull, M., and P. B. Kelemen (2001), On the conditions for lower crustal convective instability, *J. Geophys. Res.*, *106*, 6423–6446.

Kay, R. W., and S. M. Kay (1993), Delamination and delamination magmatism, *Tectonophysics*, *219*, 177–189.

Kelemen, P. B., H. J. B. Dick, and J. E. Quick (1992), Formation of harzburgite by pervasive melt/rock reaction in the upper mantle, *Nature*, *358*, 635–641.

Kelemen, P. B., G. M. Yogodzinski, and D. W. Scholl (2003), Along-strike variation in the Aleutian island arc: Genesis of high Mg# andesite and implications for continental crust, in *Inside the Subduction Factory*, *Geophys. Monogr. Ser.*, vol. 138, edited by J. Eiler, pp. 223–276, AGU, Washington, D. C.

Kelley, K. A., T. Plank, L. Farr, J. Ludden, and H. Staudigel (2005), Subduction cycling of U, Th, and Pb, *Earth Planet. Sci. Lett.*, *234*, 369–383.

Keppler, H. (1996), Constraints from the partitioning experiments on the composition of subduction-zone fluids, *Nature*, *380*, 237–240.

Klemme, S., J. D. Blundy, and B. J. Wood (2002), Experimental constraints on major and trace element partitioning during partial melting of eclogite, *Geochim. Cosmochim. Acta*, *66*, 3109–3123.

Klemme, S., S. Prowatke, K. Hametner, and D. Günther (2005), Partitioning of trace elements between rutile and silicate melts: Implications for subduction zones, *Geochim. Cosmochim. Acta*, *69*, 2361–2371.

Kogiso, T., Y. Tatsumi, and S. Nakano (1997), Trace element transport during dehydration processes in the subducted crust: 1. Experiments and implications for the origin of ocean island basalts, *Earth Planet. Sci. Lett.*, *148*, 193–205.

Lassiter, J. C., and E. H. Hauri (1998), Osmium-isotope variations in Hawaiian lavas: Evidence for recycled oceanic lithosphere in the Hawaiian plume, *Earth Planet. Sci. Lett.*, *164*, 483–496.

Le Roex, A. P., R. A. Cliff, and B. J. I. Adair (1990), Tristan da Cunha, South Atlantic: Geochemistry and petrogenesis of a basanite-phonolite lava series, *J. Petrol.*, *31*, 779–812.

McCulloch, M. T., and J. A. Gamble (1991), Geochemical and geodynamical constraints on subduction zone magmatism, *Earth Planet. Sci. Lett.*, *102*, 358–374.

McDonough, W., and S. S. Sun (1995), The composition of the Earth, *Chem. Geol.*, *120*, 223–253.

Morris, J. D., W. P. Leeman, and F. Tera (1990), The subducted component in island arc lavas: Constraints from Be isotopes and B-Be systematics, *Nature*, *344*, 31–36.

Nakamura, Y., and M. Tatsumoto (1988), Pb, Nd, and Sr isotopic evidence for a multicomponent source for rocks of Cook-Austral Islands and heterogeneities of mantle planes, *Geochim. Cosmochim. Acta*, *52*, 2909–2924.

Newsom, H. E., W. M. White, K. P. Jochum, and A. W. Hofmann (1986), Siderophile and chalcophile element abundances in oceanic basalts, Pb isotopic evolution and growth of the Earth's core, *Earth Planet. Sci. Lett.*, *80*, 299–313.

Nichols, G. T., P. J. Wyllie, and C. R. Stern (1994), Subduction zone melting of pelagic sediments constrained by melting experiments, *Nature*, *371*, 785–788.

Niu, Y., and R. Batiza (1997), Trace element evidence from seamounts for recycled oceanic crust in the Eastern Pacific mantle, *Earth Planet. Sci. Lett.*, *148*, 471–483.

Niu, Y., and M. J. O'Hara (2003), Origin of ocean island basalts: A new perspective from petrology, geochemistry, and mineral physics considerations, *J. Geophys. Res.*, *108*(B4), 2209, doi:10.1029/2002JB002048.

Niu, Y., K. D. Collerson, R. Batiza, J. I. Wendt, and M. Regelous (1999), Origin of enriched-type mid-ocean ridge basalt at ridges far from mantle plumes: The East Pacific Rise at 11°20′N, *J. Geophys. Res.*, *104*, 7067–7087.

Palacz, Z. A., and A. D. Saunders (1986), Coupled trace element and isotope enrichment in the Cook-Austral-Samoa islands, southwest Pacific, *Earth Planet. Sci. Lett.*, *79*, 270–280.

Pearce, N. J. G., W. T. Perkins, J. A. Westgate, M. P. Gorton, S. E. Jackson, C. R. Neal, and S. P. Chenery (1997), A compilation of new and published major and trace element data for NIST SRM 610 and NIST SRM 612 glass reference materials, *Geostand. Newsl.*, *21*, 115–144.

Pearson, D. G., G. J. Irvine, D. A. Ionov, F. R. Boyd, and G. E. Dreibus (2004), Re-Os isotope systematics and platinum group element fractionation during mantle melt extraction: A study of massif and xenolith peridotite suites, *Chem. Geol.*, *208*, 29–59.

Plank, T. (2005), Constraints from thorium/lanthanum on sediment recycling at subduction zones and the evolution of the continents, *J. Petrol.*, *46*, 921–944.

Plank, T., and C. H. Langmuir (1998), The chemical composition of subducting sediment and its consequences for the crust and mantle, *Chem. Geol.*, *145*, 325–394.

Raczek, I., B. Stoll, A. W. Hofmann, and K. P. Jochum (2001), High-precision trace element data for the USGS reference materials BCR-1, BCR-2, BHVO-1, BHVO-2, AGV-1, AGV-2, DTS-1, DTS-2, GSP-1 and GSP-2 by ID-TIMS and MIC-SSMS, *Geostand. Newsl.*, *25*, 77–86.

Rehkämper, M., and A. W. Hofmann (1997), Recycled ocean crust and sediment in Indian Ocean MORB, *Earth Planet. Sci. Lett.*, *147*, 93–106.

Reisberg, L., A. Zindler, F. Marcantonio, W. White, D. Wyman, and B. Weaver (1993), Os isotope systematics in ocean island basalts, *Earth Planet. Sci. Lett.*, *120*, 149–167.

Roy-Barman, M., and C. J. Allègre (1995), $^{187}Os/^{186}Os$ in oceanic basalts: Tracing oceanic crust recycling in the mantle, *Earth Planet. Sci. Lett.*, *129*, 145–161.

Rudnick, R. L. (1995), Making continental crust, *Nature*, *378*, 571–578.

Rudnick, R. L., and D. M. Fountain (1995), Nature and composition of the continental crust: A lower crustal perspective, *Rev. Geophys.*, *33*, 267–309.

Rudnick, R. L., and S. Gao (2004), Composition of the continental crust, in *Treatise on Geochemistry*, vol. 3, *The Crust*, edited by R. L. Rudnick, pp. 1–64, Elsevier, New York.

Sack, R. O., D. Walker, and I. S. E. Carmichael (1987), Experimental petrology of alkalic lavas: Constraints on cotectics of multiple saturation in natural basic lavas, *Contrib. Mineral. Petrol.*, *96*, 1–23.

Salters, V. J. M., and A. Stracke (2004), Composition of the depleted mantle, *Geochem. Geophys. Geosyst.*, *5*, Q05B07, doi:10.1029/2003GC000597.

Salters, V. J. M., and W. M. White (1998), Hf isotope constraints on mantle evolution, *Chem. Geol.*, *145*, 447–460.

Shaw, D. M. (1970), Trace element fractionation during anatexis, *Geochim. Cosmochim. Acta*, *34*, 237–243.

Shaw, D. M., A. P. Dickin, L. H. R. H. McNutt, H. P. Schwarz, and M. G. Truscott (1994), Crustal geochemistry in the Wawa-Foyelet region, Ontario, *Can. J. Earth Sci.*, *31*, 1104–1121.

Sims, K. W. W., and D. J. DePaolo (1997), Inferences about mantle magma sources from incompatible element concentration ratios in oceanic basalts, *Geochim. Cosmochim. Acta*, *61*, 765–784.

Stalder, R., S. F. Foley, G. P. Brey, and I. Horn (1998), Mineral-aqueous fluid partitioning of trace elements at 900–1200°C and 3.0–5.7 GPa: New experimental data for garnet, clinopyroxene, and rutile, and implications for mantle metasomatism, *Geochim. Cosmochim. Acta*, *62*, 1781–1801.

Staudigel, H., T. Plank, W. M. White, and H. U. Schmincke (1996), Geochemical fluxes during seafloor alteration of the basaltic upper crust: DSDP sites 417 and 418, in *Subduction: Top to Bottom*, *Geophys. Monogr. Ser.*, vol. 96, edited by G. E. Bebout et al., pp. 19–38, AGU, Washington, D. C.

Stern, C. R., and R. Kilian (1996), Role of the subducted slab, mantle wedge and continental crust in the generation of adakites from the Andean Austral Volcanic Zone, *Contrib. Mineral. Petrol.*, *123*, 263–281.

Stracke, A., M. Bizimis, and V. J. M. Salters (2003a), Recycling oceanic crust: Quantitative constraints, *Geochem. Geophys. Geosyst.*, *4*(3), 8003, doi:10.1029/2001GC000223.

Stracke, A., A. Zindler, V. J. M. Salters, D. McKenzie, J. Blichert-Toft, F. Albarède, and K. Grönvold (2003b), Theistareykir revisited, *Geochem. Geophys. Geosyst.*, *4*(2), 8507, doi:10.1029/2001GC000201.

Stracke, A., M. Willbold, and C. Hemond (2004), The origin of EM1 signatures in basalts from Tristan da Cunha and Gough, *Eos Trans. AGU*, *85*(47), Fall Meet. Suppl., Abstract V51B-0565.

Stracke, A., A. W. Hofmann, and S. R. Hart (2005), FOZO, HIMU, and the rest of the mantle zoo, *Geochem. Geophys. Geosyst.*, *6*, Q05007, doi:10.1029/2004GC000824.

Sun, S. S., and W. F. McDonough (1989), Chemical and isotopic systematics of oceanic basalts: Implications for mantle composition and processes, in *Magmatism in the Ocean Basins*, edited by A. D. Saunders and M. J. Norry, *Geol. Soc. Spec. Publ.*, *42*, 313–345.

Tatsumi, Y. (2000), Continental crust formation by crustal delamination in subduction zones and complementary accumulation of the enriched mantle I component in the mantle, *Geochem. Geophys. Geosyst.*, *1*(12), doi:10.1029/2000GC000094.

Tatsumi, Y., and T. Kogiso (1997), Trace element transport during dehydration processes in the subducted crust: 2. Origin of chemical and physical characteristics in arc magmatism, *Earth Planet. Sci. Lett.*, *148*, 207–221.

Tatsumi, Y., D. J. Hamilton, and R. W. Nesbitt (1986), Chemical characterization of fluid phase released from a subducted lithosphere and origin of arc magmas: Evidence from high-pressure experiments and natural rocks, *J. Volcanol. Geotherm. Res.*, *29*, 293–309.

Tatsumoto, M., and Y. Nakamura (1991), DUPAL anomaly in the Sea of Japan: Pb, Nd, and Sr isotope variations at the eastern Eurasian continental margin, *Geochim. Cosmochim. Acta*, *55*, 3697–3708.

Taylor, R. S., and S. M. McLennan (1985), *The Continental Crust: Its Composition and Evolution*, Blackwell, Malden, Mass.

Vannucchi, P., S. Galeotti, P. D. Clift, C. R. Ranero, and R. von Huene (2004), Long-term subduction-erosion along the Guatemalan margin of the Middle America Trench, *Geology*, *32*, 617–620.

Vidal, P., C. Chauvel, and R. Brousse (1984), Large mantle heterogeneity beneath French Polynesia, *Nature*, *307*, 536–538.

Villaseca, C., H. Downes, C. Pin, and L. Barbero (1999), Nature and composition of the lower continental crust in central Spain and the granulite-granite linkage: Inferences from granulitic xenoliths, *J. Petrol.*, *40*, 1465–1496.

von Huene, R., C. R. Ranero, and P. Vannucchi (2004), Generic model of subduction erosion, *Geology*, *32*, 913–916.

Weaver, B. L. (1991), The origin of oceanic island basalt end-member compositions: Trace element and isotopic constraints, *Earth Planet. Sci. Lett.*, *104*, 381–397.

Weaver, B. L., and J. Tarney (1984), Empirical approach to estimating the composition of the continental crust, *Nature*, *310*, 575–577.

Weis, D., F. A. Frey, H. Leyrit, and I. Gautier (1993), Kerguelen Archipelago revisited: Geochemical and isotopic study of the Southeast Province lavas, *Earth Planet. Sci. Lett.*, *118*, 101–119.

White, W. M. (1985), Sources of oceanic basalts: Radiogenic isotopic evidence, *Geology*, *13*, 115–118.

White, W. M., and R. A. Duncan (1996), Geochemistry and geochronology of the Society islands: New evidence for deep mantle recycling, in *Earth Processes: Reading the Isotopic Code*, *Geophys. Monogr. Ser.*, vol. 95, edited by A. Basu and S. Hart, pp. 183–206, AGU, Washington, D. C.

White, W. M., and B. Dupré (1986), Sediment subduction and magma genesis in the Lesser Antilles: Isotopic and trace element constraints, *J. Geophys. Res.*, *91*, 5927–5941.

White, W. M., and A. W. Hofmann (1982), Sr and Nd isotope geochemistry of oceanic basalts and mantle evolution, *Nature*, *296*, 821–825.

Willbold, M., and K. P. Jochum (2005), Multi-element isotope dilution sector field ICP-MS: A precise technique for the analysis of geological materials and its application to geological reference materials, *Geostand. Geoanal. Res.*, *29*, 63–82.

Willbold, M., K. P. Jochum, I. Raczek, M. A. Amini, B. Stoll, and A. W. Hofmann (2003), Validation of multi-element isotope dilution ICPMS for the analysis of basalts, *Anal. Bioanal. Chem.*, *377*, 117–125.

Woodhead, J. D., and C. W. Devey (1993), Geochemistry of the Pitcairn seamount, I: Source character and temporal trends, *Earth Planet. Sci. Lett.*, *116*, 81–99.

Woodhead, J. D., and M. T. McCulloch (1989), Ancient seafloor signals in Pitcairn island lavas and evidence for large amplitude, small length-scale mantle heterogeneities, *Earth Planet. Sci. Lett.*, *94*, 257–273.

Workman, R. K., S. R. Hart, M. Jackson, M. Regelous, K. A. Farley, J. Blusztajn, M. Kurz, and H. Staudigel (2004), Recycled metasomatized lithosphere as the origin of the Enriched Mantle II (EM2) end-member: Evidence from the Samoan Volcanic Chain, *Geochem. Geophys. Geosyst.*, *5*, Q04008, doi:10.1029/2003GC000623.

Wright, E., and W. M. White (1987), The origin of Samoa: New evidence from Sr, Nd, and Pb isotopes, *Earth Planet. Sci. Lett.*, *81*, 151–162.

Zindler, A., and S. Hart (1986), Chemical geodynamics, *Annu. Rev. Earth Planet. Sci.*, *14*, 493–571.